

BOILING AND CONDENSATION

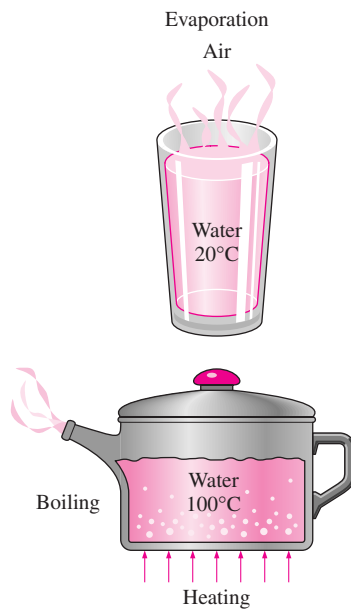
We know from thermodynamics that when the temperature of a liquid at a specified pressure is raised to the saturation temperature T_{sat} at that pressure, *boiling* occurs. Likewise, when the temperature of a vapor is lowered to T_{sat} , *condensation* occurs. In this chapter we study the rates of heat transfer during such liquid-to-vapor and vapor-to-liquid phase transformations.

Although boiling and condensation exhibit some unique features, they are considered to be forms of *convection* heat transfer since they involve fluid motion (such as the rise of the bubbles to the top and the flow of condensate to the bottom). Boiling and condensation differ from other forms of convection in that they depend on the *latent heat of vaporization* h_{fg} of the fluid and the *surface tension* σ at the liquid–vapor interface, in addition to the properties of the fluid in each phase. Noting that under equilibrium conditions the temperature remains constant during a phase-change process at a fixed pressure, large amounts of heat (due to the large latent heat of vaporization released or absorbed) can be transferred during boiling and condensation essentially at constant temperature. In practice, however, it is necessary to maintain some difference between the surface temperature T_s and T_{sat} for effective heat transfer. Heat transfer coefficients h associated with boiling and condensation are typically much higher than those encountered in other forms of convection processes that involve a single phase.

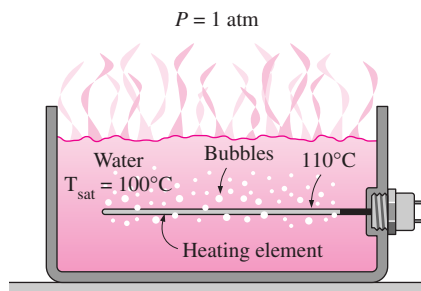
We start this chapter with a discussion of the *boiling curve* and the modes of pool boiling such as *free convection boiling*, *nucleate boiling*, and *film boiling*. We then discuss boiling in the presence of forced convection. In the second part of this chapter, we describe the physical mechanism of *film condensation* and discuss condensation heat transfer in several geometrical arrangements and orientations. Finally, we introduce *dropwise condensation* and discuss ways of maintaining it.

CONTENTS

10–1	Boiling Heat Transfer	516
10–2	Pool Boiling	518
10–3	Flow Boiling	530
10–4	Condensation Heat Transfer	532
10–5	Film Condensation	532
10–6	Film Condensation Inside Horizontal Tubes	545
10–7	Dropwise Condensation	545
	<i>Topic of Special Interest:</i> Heat Pipes	546

**FIGURE 10-1**

A liquid-to-vapor phase change process is called *evaporation* if it occurs at a liquid–vapor interface and *boiling* if it occurs at a solid–liquid interface.

**FIGURE 10-2**

Boiling occurs when a liquid is brought into contact with a surface at a temperature above the saturation temperature of the liquid.

10-1 ■ BOILING HEAT TRANSFER

Many familiar engineering applications involve condensation and boiling heat transfer. In a household refrigerator, for example, the refrigerant absorbs heat from the refrigerated space by boiling in the *evaporator* section and rejects heat to the kitchen air by condensing in the *condenser* section (the long coils behind the refrigerator). Also, in steam power plants, heat is transferred to the steam in the *boiler* where water is vaporized, and the waste heat is rejected from the steam in the *condenser* where the steam is condensed. Some electronic components are cooled by boiling by immersing them in a fluid with an appropriate boiling temperature.

Boiling is a liquid-to-vapor phase change process just like evaporation, but there are significant differences between the two. **Evaporation** occurs at the *liquid–vapor interface* when the vapor pressure is less than the saturation pressure of the liquid at a given temperature. Water in a lake at 20°C, for example, will evaporate to air at 20°C and 60 percent relative humidity since the saturation pressure of water at 20°C is 2.3 kPa and the vapor pressure of air at 20°C and 60 percent relative humidity is 1.4 kPa (evaporation rates are determined in Chapter 14). Other examples of evaporation are the drying of clothes, fruits, and vegetables; the evaporation of sweat to cool the human body; and the rejection of waste heat in wet cooling towers. Note that evaporation involves no bubble formation or bubble motion (Fig. 10–1).

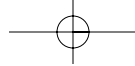
Boiling, on the other hand, occurs at the *solid–liquid interface* when a liquid is brought into contact with a surface maintained at a temperature T_s sufficiently above the saturation temperature T_{sat} of the liquid (Fig. 10–2). At 1 atm, for example, liquid water in contact with a solid surface at 110°C will boil since the saturation temperature of water at 1 atm is 100°C. The boiling process is characterized by the rapid formation of *vapor bubbles* at the solid–liquid interface that detach from the surface when they reach a certain size and attempt to rise to the free surface of the liquid. When cooking, we do not say water is boiling until we see the bubbles rising to the top. Boiling is a complicated phenomenon because of the large number of variables involved in the process and the complex fluid motion patterns caused by the bubble formation and growth.

As a form of convection heat transfer, the *boiling heat flux* from a solid surface to the fluid is expressed from Newton’s law of cooling as

$$\dot{q}_{\text{boiling}} = h(T_s - T_{\text{sat}}) = h\Delta T_{\text{excess}} \quad (\text{W/m}^2) \quad (10-1)$$

where $\Delta T_{\text{excess}} = T_s - T_{\text{sat}}$ is called the *excess temperature*, which represents the excess of the surface above the saturation temperature of the fluid.

In the preceding chapters we considered forced and free convection heat transfer involving a single phase of a fluid. The analysis of such convection processes involves the thermophysical properties ρ , μ , k , and C_p of the fluid. The analysis of boiling heat transfer involves these properties of the liquid (indicated by the subscript l) or vapor (indicated by the subscript v) as well as the properties h_{fg} (the latent heat of vaporization) and σ (the surface tension). The h_{fg} represents the energy absorbed as a unit mass of liquid vaporizes at a specified temperature or pressure and is the primary quantity of energy



transferred during boiling heat transfer. The h_{fg} values of water at various temperatures are given in Table A-9.

Bubbles owe their existence to the *surface-tension* σ at the liquid–vapor interface due to the attraction force on molecules at the interface toward the liquid phase. The surface tension decreases with increasing temperature and becomes zero at the critical temperature. This explains why no bubbles are formed during boiling at supercritical pressures and temperatures. Surface tension has the unit N/m.

The boiling processes in practice do not occur under *equilibrium* conditions, and normally the bubbles are not in thermodynamic equilibrium with the surrounding liquid. That is, the temperature and pressure of the vapor in a bubble are usually different than those of the liquid. The pressure difference between the liquid and the vapor is balanced by the surface tension at the interface. The temperature difference between the vapor in a bubble and the surrounding liquid is the driving force for heat transfer between the two phases. When the liquid is at a *lower temperature* than the bubble, heat will be transferred from the bubble into the liquid, causing some of the vapor inside the bubble to condense and the bubble to collapse eventually. When the liquid is at a *higher temperature* than the bubble, heat will be transferred from the liquid to the bubble, causing the bubble to grow and rise to the top under the influence of buoyancy.

Boiling is classified as *pool boiling* or *flow boiling*, depending on the presence of bulk fluid motion (Fig. 10–3). Boiling is called **pool boiling** in the absence of bulk fluid flow and **flow boiling** (or *forced convection boiling*) in the presence of it. In pool boiling, the fluid is stationary, and any motion of the fluid is due to natural convection currents and the motion of the bubbles under the influence of buoyancy. The boiling of water in a pan on top of a stove is an example of pool boiling. Pool boiling of a fluid can also be achieved by placing a heating coil in the fluid. In flow boiling, the fluid is forced to move in a heated pipe or over a surface by external means such as a pump. Therefore, flow boiling is always accompanied by other convection effects.

Pool and flow boiling are further classified as *subcooled boiling* or *saturated boiling*, depending on the bulk liquid temperature (Fig. 10–4). Boiling is said to be **subcooled** (or *local*) when the temperature of the main body of the liquid is below the saturation temperature T_{sat} (i.e., the bulk of the liquid is subcooled) and **saturated** (or *bulk*) when the temperature of the liquid is equal to T_{sat} (i.e., the bulk of the liquid is saturated). At the early stages of boiling, the bubbles are confined to a narrow region near the hot surface. This is because the liquid adjacent to the hot surface vaporizes as a result of being heated above its saturation temperature. But these bubbles disappear soon after they move away from the hot surface as a result of heat transfer from the bubbles to the cooler liquid surrounding them. This happens when the bulk of the liquid is at a lower temperature than the saturation temperature. The bubbles serve as “energy movers” from the hot surface into the liquid body by absorbing heat from the hot surface and releasing it into the liquid as they condense and collapse. Boiling in this case is confined to a region in the locality of the hot surface and is appropriately called *local* or *subcooled* boiling. When the entire liquid body reaches the saturation temperature, the bubbles start rising to the top. We can see bubbles throughout the bulk of the liquid,

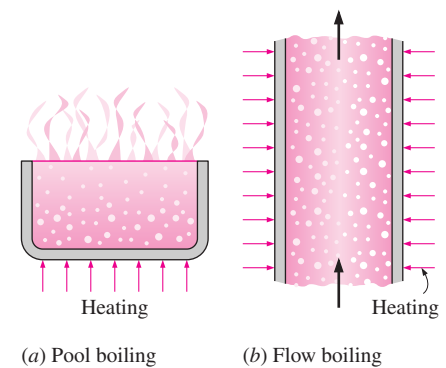


FIGURE 10–3

Classification of boiling on the basis of the presence of bulk fluid motion.

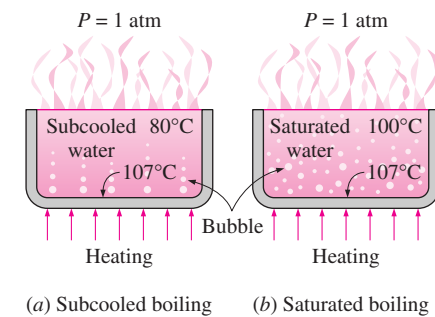
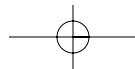


FIGURE 10–4

Classification of boiling on the basis of the presence of bulk liquid temperature.



and boiling in this case is called the *bulk* or *saturated* boiling. Next, we consider different boiling regimes in detail.

10-2 ■ POOL BOILING

So far we presented some general discussions on boiling. Now we turn our attention to the physical mechanisms involved in *pool boiling*, that is, the boiling of stationary fluids. In pool boiling, the fluid is not forced to flow by a mover such as a pump, and any motion of the fluid is due to natural convection currents and the motion of the bubbles under the influence of buoyancy.

As a familiar example of pool boiling, consider the boiling of tap water in a pan on top of a stove. The water will initially be at about 15°C, far below the saturation temperature of 100°C at standard atmospheric pressure. At the early stages of boiling, you will not notice anything significant except some bubbles that stick to the surface of the pan. These bubbles are caused by the release of air molecules dissolved in liquid water and should not be confused with vapor bubbles. As the water temperature rises, you will notice chunks of liquid water rolling up and down as a result of natural convection currents, followed by the first vapor bubbles forming at the bottom surface of the pan. These bubbles get smaller as they detach from the surface and start rising, and eventually collapse in the cooler water above. This is *subcooled boiling* since the bulk of the liquid water has not reached saturation temperature yet. The intensity of bubble formation increases as the water temperature rises further, and you will notice waves of vapor bubbles coming from the bottom and rising to the top when the water temperature reaches the saturation temperature (100°C at standard atmospheric conditions). This full scale boiling is the *saturated boiling*.

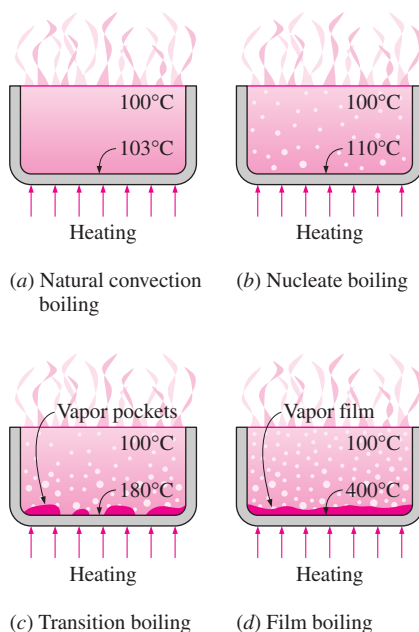


FIGURE 10-5
Different boiling regimes
in pool boiling.

Boiling Regimes and the Boiling Curve

Boiling is probably the most familiar form of heat transfer, yet it remains to be the least understood form. After hundreds of papers written on the subject, we still do not fully understand the process of bubble formation and we must still rely on empirical or semi-empirical relations to predict the rate of boiling heat transfer.

The pioneering work on boiling was done in 1934 by S. Nukiyama, who used electrically heated nichrome and platinum wires immersed in liquids in his experiments. Nukiyama noticed that boiling takes different forms, depending on the value of the excess temperature ΔT_{excess} . Four different boiling regimes are observed: *natural convection boiling*, *nucleate boiling*, *transition boiling*, and *film boiling* (Fig. 10-5). These regimes are illustrated on the **boiling curve** in Figure 10-6, which is a plot of boiling heat flux versus the excess temperature. Although the boiling curve given in this figure is for water, the general shape of the boiling curve remains the same for different fluids. The specific shape of the curve depends on the fluid–heating surface material combination and the fluid pressure, but it is practically independent of the geometry of the heating surface. We will describe each boiling regime in detail.

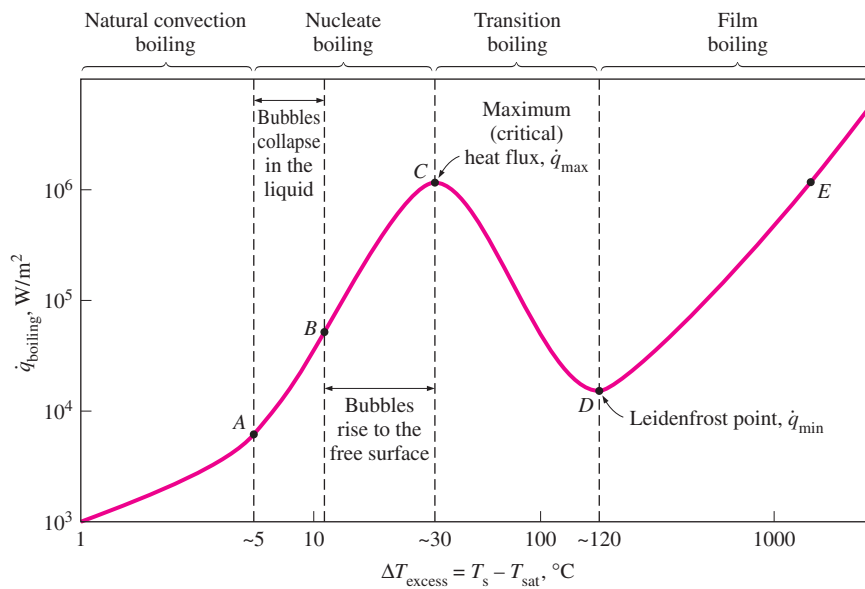


FIGURE 10-6
Typical boiling curve for water at 1 atm pressure.

Natural Convection Boiling (to Point A on the Boiling Curve)

We learned in thermodynamics that a pure substance at a specified pressure starts boiling when it reaches the saturation temperature at that pressure. But in practice we do not see any bubbles forming on the heating surface until the liquid is heated a few degrees above the saturation temperature (about 2 to 6°C for water). Therefore, the liquid is slightly *superheated* in this case (a *metastable* condition) and evaporates when it rises to the free surface. The fluid motion in this mode of boiling is governed by natural convection currents, and heat transfer from the heating surface to the fluid is by natural convection.

Nucleate Boiling (between Points A and C)

The first bubbles start forming at point A of the boiling curve at various preferential sites on the heating surface. The bubbles form at an increasing rate at an increasing number of nucleation sites as we move along the boiling curve toward point C.

The nucleate boiling regime can be separated into two distinct regions. In region A–B, *isolated bubbles* are formed at various preferential nucleation sites on the heated surface. But these bubbles are dissipated in the liquid shortly after they separate from the surface. The space vacated by the rising bubbles is filled by the liquid in the vicinity of the heater surface, and the process is repeated. The stirring and agitation caused by the entrainment of the liquid to the heater surface is primarily responsible for the increased heat transfer coefficient and heat flux in this region of nucleate boiling.

In region B–C, the heater temperature is further increased, and bubbles form at such great rates at such a large number of nucleation sites that they form numerous *continuous columns of vapor* in the liquid. These bubbles move all the way up to the free surface, where they break up and release their vapor content. The large heat fluxes obtainable in this region are caused by the combined effect of liquid entrainment and evaporation.

At large values of ΔT_{excess} , the rate of evaporation at the heater surface reaches such high values that a large fraction of the heater surface is covered by bubbles, making it difficult for the liquid to reach the heater surface and wet it. Consequently, the heat flux increases at a lower rate with increasing ΔT_{excess} , and reaches a maximum at point *C*. The heat flux at this point is called the **critical** (or **maximum**) **heat flux**, \dot{q}_{max} . For water, the critical heat flux exceeds 1 MW/m^2 .

Nucleate boiling is the most desirable boiling regime in practice because high heat transfer rates can be achieved in this regime with relatively small values of ΔT_{excess} , typically under 30°C for water. The photographs in Figure 10–7 show the nature of bubble formation and bubble motion associated with nucleate, transition, and film boiling.

Transition Boiling (between Points *C* and *D* on the Boiling Curve)

As the heater temperature and thus the ΔT_{excess} is increased past point *C*, the heat flux decreases, as shown in Figure 10–6. This is because a large fraction of the heater surface is covered by a vapor film, which acts as an insulation due to the low thermal conductivity of the vapor relative to that of the liquid. In the transition boiling regime, both nucleate and film boiling partially occur. Nucleate boiling at point *C* is completely replaced by film boiling at point *D*. Operation in the transition boiling regime, which is also called the *unstable film boiling regime*, is avoided in practice. For water, transition boiling occurs over the excess temperature range from about 30°C to about 120°C .

Film Boiling (beyond Point *D*)

In this region the heater surface is completely covered by a continuous stable vapor film. Point *D*, where the heat flux reaches a minimum, is called the **Leidenfrost point**, in honor of J. C. Leidenfrost, who observed in 1756 that liquid droplets on a very hot surface jump around and slowly boil away. The presence of a vapor film between the heater surface and the liquid is responsible for the low heat transfer rates in the film boiling region. The heat transfer rate increases with increasing excess temperature as a result of heat transfer from the heated surface to the liquid through the vapor film by radiation, which becomes significant at high temperatures.

A typical boiling process will not follow the boiling curve beyond point *C*, as Nukiyama has observed during his experiments. Nukiyama noticed, with surprise, that when the power applied to the nichrome wire immersed in water exceeded \dot{q}_{max} even slightly, the wire temperature increased suddenly to the melting point of the wire and *burnout* occurred beyond his control. When he repeated the experiments with platinum wire, which has a much higher melting point, he was able to avoid burnout and maintain heat fluxes higher than \dot{q}_{max} . When he gradually reduced power, he obtained the cooling curve shown in Figure 10–8 with a sudden drop in excess temperature when \dot{q}_{min} is reached. Note that the boiling process cannot follow the transition boiling part of the boiling curve past point *C* unless the power applied is reduced suddenly.

The *burnout phenomenon* in boiling can be explained as follows: In order to move beyond point *C* where \dot{q}_{max} occurs, we must increase the heater surface temperature T_s . To increase T_s , however, we must increase the heat flux. But

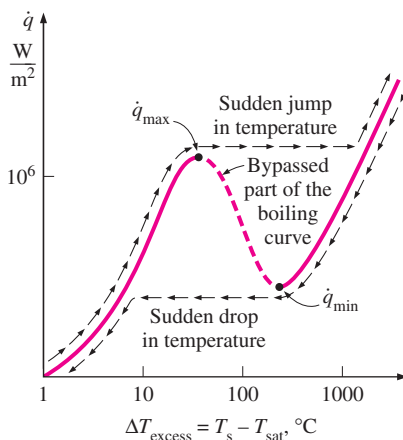
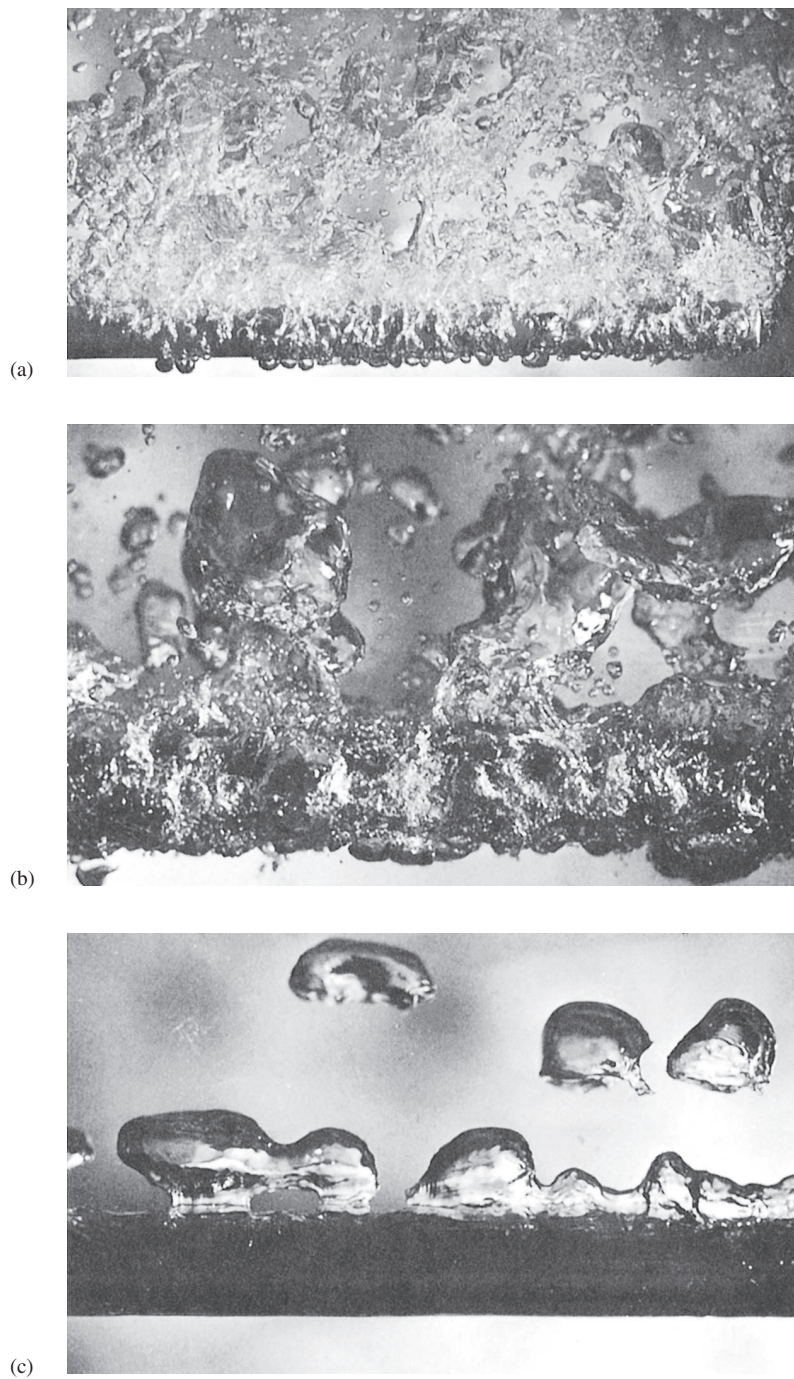
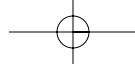


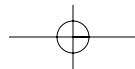
FIGURE 10–8

The actual boiling curve obtained with heated platinum wire in water as the heat flux is increased and then decreased.

**FIGURE 10-7**

Various boiling regimes during boiling of methanol on a horizontal 1-cm-diameter steam-heated copper tube: (a) nucleate boiling, (b) transition boiling, and (c) film boiling (from J. W. Westwater and J. G. Santangelo, University of Illinois at Champaign-Urbana).

the fluid cannot receive this increased energy at an excess temperature just beyond point *C*. Therefore, the heater surface ends up absorbing the increased energy, causing the heater surface temperature T_s to rise. But the fluid can receive even less energy at this increased excess temperature, causing the heater surface temperature T_s to rise even further. This continues until the surface



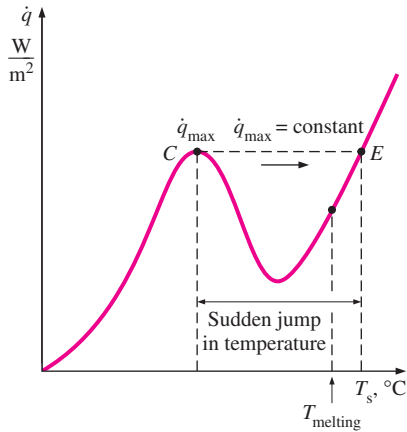


FIGURE 10-9

An attempt to increase the boiling heat flux beyond the *critical* value often causes the temperature of the heating element to jump suddenly to a value that is above the melting point, resulting in *burnout*.

temperature reaches a point at which it no longer rises and the heat supplied can be transferred to the fluid steadily. This is point *E* on the boiling curve, which corresponds to very high surface temperatures. Therefore, any attempt to increase the heat flux beyond \dot{q}_{\max} will cause the operation point on the boiling curve to jump suddenly from point *C* to point *E*. However, surface temperature that corresponds to point *E* is beyond the melting point of most heater materials, and *burnout* occurs. Therefore, point *C* on the boiling curve is also called the **burnout point**, and the heat flux at this point the **burnout heat flux** (Fig. 10-9).

Most boiling heat transfer equipment in practice operate slightly below \dot{q}_{\max} to avoid any disastrous burnout. However, in cryogenic applications involving fluids with very low boiling points such as oxygen and nitrogen, point *E* usually falls below the melting point of the heater materials, and steady film boiling can be used in those cases without any danger of burnout.

Heat Transfer Correlations in Pool Boiling

Boiling regimes discussed above differ considerably in their character, and thus different heat transfer relations need to be used for different boiling regimes. In the *natural convection boiling* regime, boiling is governed by natural convection currents, and heat transfer rates in this case can be determined accurately using natural convection relations presented in Chapter 9.

Nucleate Boiling

In the *nucleate boiling* regime, the rate of heat transfer strongly depends on the nature of nucleation (the number of active nucleation sites on the surface, the rate of bubble formation at each site, etc.), which is difficult to predict. The type and the condition of the heated surface also affect the heat transfer. These complications made it difficult to develop theoretical relations for heat transfer in the nucleate boiling regime, and people had to rely on relations based on experimental data. The most widely used correlation for the rate of heat transfer in the nucleate boiling regime was proposed in 1952 by Rohsenow, and expressed as

$$\dot{q}_{\text{nucleate}} = \mu_l h_{fg} \left[\frac{g(\rho_l - \rho_v)}{\sigma} \right]^{1/2} \left[\frac{C_p(T_s - T_{\text{sat}})}{C_{sf} h_{fg} \text{Pr}_l^n} \right]^3 \quad (10-2)$$

where

$\dot{q}_{\text{nucleate}}$ = nucleate boiling heat flux, W/m²

μ_l = viscosity of the liquid, kg/m · s

h_{fg} = enthalpy of vaporization, J/kg

g = gravitational acceleration, m/s²

ρ_l = density of the liquid, kg/m³

ρ_v = density of the vapor, kg/m³

σ = surface tension of liquid–vapor interface, N/m

C_{pl} = specific heat of the liquid, J/kg · °C

T_s = surface temperature of the heater, °C

T_{sat} = saturation temperature of the fluid, °C

C_{sf} = experimental constant that depends on surface–fluid combination

Pr_l = Prandtl number of the liquid

n = experimental constant that depends on the fluid

It can be shown easily that using property values in the specified units in the Rohsenow equation produces the desired unit W/m^2 for the boiling heat flux, thus saving one from having to go through tedious unit manipulations (Fig. 10–10).

The surface tension at the vapor–liquid interface is given in Table 10–1 for water, and Table 10–2 for some other fluids. Experimentally determined values of the constant C_{sf} are given in Table 10–3 for various fluid–surface combinations. These values can be used for *any geometry* since it is found that the rate of heat transfer during nucleate boiling is essentially independent of the geometry and orientation of the heated surface. The fluid properties in Eq. 10–2 are to be evaluated at the saturation temperature T_{sat} .

The *condition* of the heater surface greatly affects heat transfer, and the Rohsenow equation given above is applicable to *clean* and relatively *smooth* surfaces. The results obtained using the Rohsenow equation can be in error by $\pm 100\%$ for the heat transfer rate for a given excess temperature and by $\pm 30\%$ for the excess temperature for a given heat transfer rate. Therefore, care should be exercised in the interpretation of the results.

Recall from thermodynamics that the enthalpy of vaporization h_{fg} of a pure substance decreases with increasing pressure (or temperature) and reaches zero at the critical point. Noting that h_{fg} appears in the denominator of the Rohsenow equation, we should see a significant rise in the rate of heat transfer at *high pressures* during nucleate boiling.

Peak Heat Flux

In the design of boiling heat transfer equipment, it is extremely important for the designer to have a knowledge of the maximum heat flux in order to avoid the danger of burnout. The *maximum* (or *critical*) *heat flux* in nucleate pool boiling was determined theoretically by S. S. Kutateladze in Russia in 1948 and N. Zuber in the United States in 1958 using quite different approaches, and is expressed as (Fig. 10–11)

$$\dot{q}_{\text{max}} = C_{cr} h_{fg} [\sigma g \rho_v^2 (\rho_l - \rho_v)]^{1/4} \quad (10-3)$$

where C_{cr} is a constant whose value depends on the heater geometry. Exhaustive experimental studies by Lienhard and his coworkers indicated that the value of C_{cr} is about 0.15. Specific values of C_{cr} for different heater geometries are listed in Table 10–4. Note that the heaters are classified as being large or small based on the value of the parameter L^* .

Equation 10–3 will give the maximum heat flux in W/m^2 if the properties are used *in the units specified* earlier in their descriptions following Eq. 10–2. The maximum heat flux is independent of the fluid–heating surface combination, as well as the viscosity, thermal conductivity, and the specific heat of the liquid.

Note that ρ_v increases but σ and h_{fg} decrease with increasing pressure, and thus the change in \dot{q}_{max} with pressure depends on which effect dominates. The experimental studies of Cichelli and Bonilla indicate that \dot{q}_{max} increases with pressure up to about one-third of the critical pressure, and then starts to decrease and becomes zero at the critical pressure. Also note that \dot{q}_{max} is proportional to h_{fg} , and large maximum heat fluxes can be obtained using fluids with a large enthalpy of vaporization, such as water.

$$\begin{aligned} \dot{q} &= \left(\frac{\text{kg}}{\text{m} \cdot \text{s}} \right) \left(\frac{\text{J}}{\text{kg}} \right) \\ &\times \left(\frac{\text{m kg}}{\text{s}^2 \text{m}^3} \right)^{1/2} \left(\frac{\text{J}}{\text{kg} \cdot ^\circ\text{C}} \right)^3 \\ &= \frac{\text{W}}{\text{m}} \left(\frac{1}{\text{m}^2} \right)^{1/2} (1)^3 \\ &= \text{W}/\text{m}^2 \end{aligned}$$

FIGURE 10–10

Equation 10–2 gives the boiling heat flux in W/m^2 when the quantities are expressed in the units specified in their descriptions.

TABLE 10–1

Surface tension of liquid–vapor interface for water

$T, ^\circ\text{C}$	$\sigma, \text{N}/\text{m}^*$
0	0.0757
20	0.0727
40	0.0696
60	0.0662
80	0.0627
100	0.0589
120	0.0550
140	0.0509
160	0.0466
180	0.0422
200	0.0377
220	0.0331
240	0.0284
260	0.0237
280	0.0190
300	0.0144
320	0.0099
340	0.0056
360	0.0019
374	0.0

*Multiply by 0.06852 to convert to lb/ft or by 2.2046 to convert to lbm/s^2 .

TABLE 10-2

Surface tension of some fluids (from Suryanarayana, Ref. 26; originally based on data from Jasper, Ref. 14)

Substance and Temp. Range	Surface Tension, σ , N/m* (T in °C)
Ammonia, -75 to -40°C:	$0.0264 + 0.000223T$
Benzene, 10 to 80°C:	$0.0315 - 0.000129T$
Butane, -70 to -20°C:	$0.0149 - 0.000121T$
Carbon dioxide, -30 to -20°C:	$0.0043 - 0.000160T$
Ethyl alcohol, 10 to 70°C:	$0.0241 - 0.000083T$
Mercury, 5 to 200°C:	$0.4906 - 0.000205T$
Methyl alcohol, 10 to 60°C:	$0.0240 - 0.000077T$
Pentane, 10 to 30°C:	$0.0183 - 0.000110T$
Propane, -90 to -10°C:	$0.0092 - 0.000087T$

*Multiply by 0.06852 to convert to lbf/ft or by 2.2046 to convert to lbm/s².

TABLE 10-3

Values of the coefficient C_{sf} and n for various fluid-surface combinations

Fluid-Heating Surface Combination	C_{sf}	n
Water-copper (polished)	0.0130	1.0
Water-copper (scored)	0.0068	1.0
Water-stainless steel (mechanically polished)	0.0130	1.0
Water-stainless steel (ground and polished)	0.0060	1.0
Water-stainless steel (teflon pitted)	0.0058	1.0
Water-stainless steel (chemically etched)	0.0130	1.0
Water-brass	0.0060	1.0
Water-nickel	0.0060	1.0
Water-platinum	0.0130	1.0
<i>n</i> -Pentane-copper (polished)	0.0154	1.7
<i>n</i> -Pentane-chromium	0.0150	1.7
Benzene-chromium	0.1010	1.7
Ethyl alcohol-chromium	0.0027	1.7
Carbon tetrachloride-copper	0.0130	1.7
Isopropanol-copper	0.0025	1.7

Minimum Heat Flux

Minimum heat flux, which occurs at the Leidenfrost point, is of practical interest since it represents the lower limit for the heat flux in the film boiling regime. Using the stability theory, Zuber derived the following expression for the minimum heat flux for a large horizontal plate,

$$\dot{q}_{\min} = 0.09\rho_v h_{fg} \left[\frac{\sigma g(\rho_l - \rho_v)}{(\rho_l + \rho_v)^2} \right]^{1/4} \quad (10-4)$$

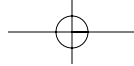
where the constant 0.09 was determined by Berenson in 1961. He replaced the theoretically determined value of $\frac{\pi}{24}$ by 0.09 to match the experimental data better. Still, the relation above can be in error by 50 percent or more.

TABLE 10-4

Values of the coefficient C_{cr} for use in Eq. 10-3 for maximum heat flux (dimensionless parameter $L^* = L[g(\rho_l - \rho_v)/\sigma]^{1/2}$)

Heater Geometry	C_{cr}	Charac. Dimension of Heater, L	Range of L^*
Large horizontal flat heater	0.149	Width or diameter	$L^* > 27$
Small horizontal flat heater ¹	$18.9K_1$	Width or diameter	$9 < L^* < 20$
Large horizontal cylinder	0.12	Radius	$L^* > 1.2$
Small horizontal cylinder	$0.12L^{*-0.25}$	Radius	$0.15 < L^* < 1.2$
Large sphere	0.11	Radius	$L^* > 4.26$
Small sphere	$0.227L^{*-0.5}$	Radius	$0.15 < L^* < 4.26$

¹ $K_1 = \sigma/[g(\rho_l - \rho_v)A_{\text{heater}}]$



Film Boiling

Using an analysis similar to Nusselt's theory on filmwise condensation presented in the next section, Bromley developed a theory for the prediction of heat flux for stable *film boiling* on the outside of a horizontal cylinder. The heat flux for film boiling on a *horizontal cylinder* or *sphere* of diameter D is given by

$$\dot{q}_{\text{film}} = C_{\text{film}} \left[\frac{g k_v^3 \rho_v (\rho_l - \rho_v) [h_{fg} + 0.4 C_{pv} (T_s - T_{\text{sat}})]^{1/4}}{\mu_v D (T_s - T_{\text{sat}})} \right] (T_s - T_{\text{sat}}) \quad (10-5)$$

where k_v is the thermal conductivity of the vapor in $\text{W/m} \cdot ^\circ\text{C}$ and

$$C_{\text{film}} = \begin{cases} 0.62 & \text{for horizontal cylinders} \\ 0.67 & \text{for spheres} \end{cases}$$

Other properties are as listed before in connection with Eq. 10-2. We used a modified latent heat of vaporization in Eq. 10-5 to account for the heat transfer associated with the superheating of the vapor.

The *vapor* properties are to be evaluated at the *film temperature*, given as $T_f = (T_s + T_{\text{sat}})/2$, which is the *average temperature* of the vapor film. The liquid properties and h_{fg} are to be evaluated at the saturation temperature at the specified pressure. Again, this relation will give the film boiling heat flux in W/m^2 if the properties are used *in the units specified* earlier in their descriptions following Eq. 10-2.

At high surface temperatures (typically above 300°C), heat transfer across the vapor film by *radiation* becomes significant and needs to be considered (Fig. 10-12). Treating the vapor film as a transparent medium sandwiched between two large parallel plates and approximating the liquid as a blackbody, *radiation heat transfer* can be determined from

$$\dot{q}_{\text{rad}} = \varepsilon \sigma (T_s^4 - T_{\text{sat}}^4) \quad (10-6)$$

where ε is the emissivity of the heating surface and $\sigma = 5.67 \times 10^{-8} \text{ W/m}^2 \cdot \text{K}^4$ is the Stefan–Boltzman constant. Note that the temperature in this case *must* be expressed in K, not $^\circ\text{C}$, and that surface tension and the Stefan–Boltzman constant share the same symbol.

You may be tempted to simply add the convection and radiation heat transfers to determine the total heat transfer during film boiling. However, these two mechanisms of heat transfer adversely affect each other, causing the total heat transfer to be less than their sum. For example, the radiation heat transfer from the surface to the liquid enhances the rate of evaporation, and thus the thickness of the vapor film, which impedes convection heat transfer. For $\dot{q}_{\text{rad}} < \dot{q}_{\text{film}}$, Bromley determined that the relation

$$\dot{q}_{\text{total}} = \dot{q}_{\text{film}} + \frac{3}{4} \dot{q}_{\text{rad}} \quad (10-7)$$

correlates experimental data well.

Operation in the *transition boiling* regime is normally avoided in the design of heat transfer equipment, and thus no major attempt has been made to develop general correlations for boiling heat transfer in this regime.

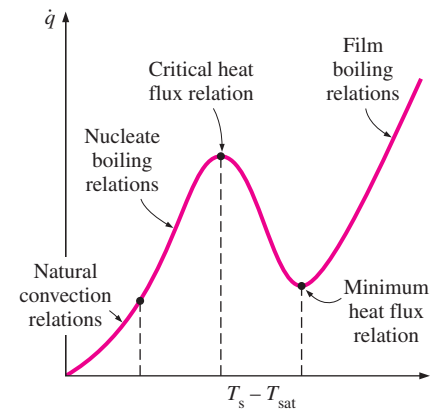


FIGURE 10-11

Different relations are used to determine the heat flux in different boiling regimes.

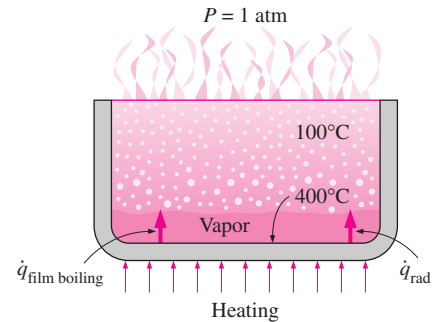


FIGURE 10-12

At high heater surface temperatures, radiation heat transfer becomes significant during film boiling.

Note that the gravitational acceleration g , whose value is approximately 9.81 m/s^2 at sea level, appears in all of the relations above for boiling heat transfer. The effects of low and high gravity (as encountered in aerospace applications and turbomachinery) are studied experimentally. The studies confirm that the critical heat flux and heat flux in film boiling are proportional to $g^{1/4}$. However, they indicate that heat flux in nucleate boiling is practically independent of gravity g , instead of being proportional to $g^{1/2}$, as dictated by Eq. 10-2.

Enhancement of Heat Transfer in Pool Boiling

The pool boiling heat transfer relations given above apply to smooth surfaces. Below we will discuss some methods to enhance heat transfer in pool boiling.

We pointed out earlier that the rate of heat transfer in the *nucleate boiling* regime strongly depends on the number of active nucleation sites on the surface, and the rate of bubble formation at each site. Therefore, any modification that will enhance *nucleation* on the heating surface will also enhance *heat transfer* in nucleate boiling. It is observed that *irregularities* on the heating surface, including roughness and dirt, serve as additional nucleation sites during boiling, as shown in Figure 10-13. For example, the first bubbles in a pan filled with water are most likely to form at the *scratches* at the bottom surface. These scratches act like “nests” for the bubbles to form and thus increase the rate of bubble formation. Berensen has shown that heat flux in the nucleate boiling regime can be increased by a factor of 10 by *roughening* the heating surface. However, these high heat transfer rates cannot be sustained for long since the effect of surface roughness is observed to decay with time, and the heat flux to drop eventually to values encountered on smooth surfaces. The effect of surface roughness is negligible on the critical heat flux and the heat flux in film boiling.

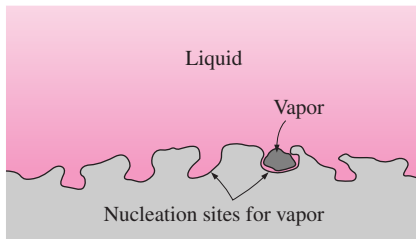


FIGURE 10-13

The cavities on a rough surface act as nucleation sites and enhance boiling heat transfer.

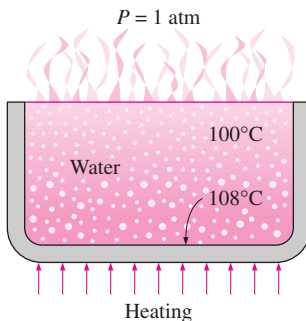


FIGURE 10-15

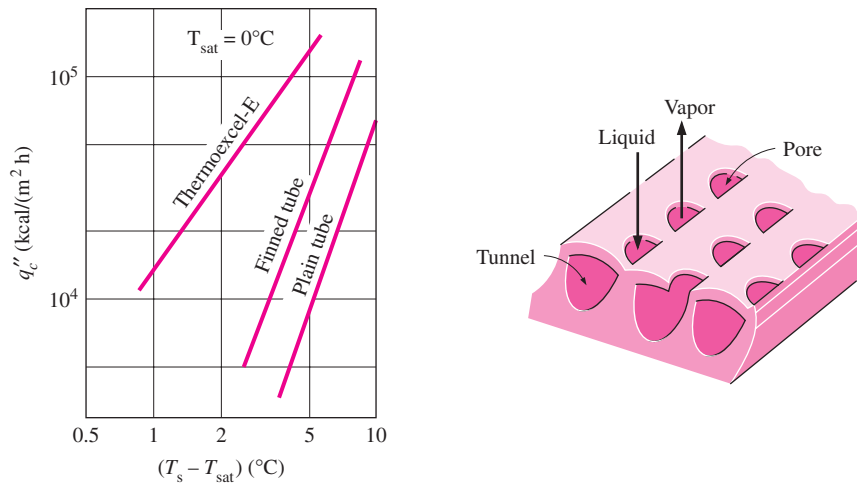
Schematic for Example 10-1.

Surfaces that provide enhanced heat transfer in nucleate boiling *permanently* are being manufactured and are available in the market. Enhancement in nucleation and thus heat transfer in such special surfaces is achieved either by *coating* the surface with a thin layer (much less than 1 mm) of very porous material or by *forming cavities* on the surface mechanically to facilitate continuous vapor formation. Such surfaces are reported to enhance heat transfer in the nucleate boiling regime by a factor of up to 10, and the critical heat flux by a factor of 3. The enhancement provided by one such material prepared by machine roughening, the thermoexcel-E, is shown in Figure 10-14. The use of finned surfaces is also known to enhance nucleate boiling heat transfer and the critical heat flux.

Boiling heat transfer can also be enhanced by other techniques such as *mechanical agitation* and *surface vibration*. These techniques are not practical, however, because of the complications involved.

EXAMPLE 10-1 Nucleate Boiling of Water in a Pan

Water is to be boiled at atmospheric pressure in a mechanically polished stainless steel pan placed on top of a heating unit, as shown in Figure 10-15. The inner surface of the bottom of the pan is maintained at 108°C . If the diameter of the bottom of the pan is 30 cm, determine (a) the rate of heat transfer to the water and (b) the rate of evaporation of water.

**FIGURE 10-14**

The enhancement of boiling heat transfer in Freon-12 by a mechanically roughened surface, thermoexcel-E.

SOLUTION Water is boiled at 1 atm pressure on a stainless steel surface. The rate of heat transfer to the water and the rate of evaporation of water are to be determined.

Assumptions 1 Steady operating conditions exist. 2 Heat losses from the heater and the pan are negligible.

Properties The properties of water at the saturation temperature of 100°C are $\sigma = 0.0589$ N/m (Table 10-1) and, from Table A-9,

$$\begin{aligned} \rho_l &= 957.9 \text{ kg/m}^3 & h_{fg} &= 2257.0 \times 10^3 \text{ J/kg} \\ \rho_v &= 0.6 \text{ kg/m}^3 & \mu_l &= 0.282 \times 10^{-3} \text{ kg} \cdot \text{m/s} \\ \text{Pr}_l &= 1.75 & C_{pl} &= 4217 \text{ J/kg} \cdot ^\circ\text{C} \end{aligned}$$

Also, $C_{sf} = 0.0130$ and $n = 1.0$ for the boiling of water on a mechanically polished stainless steel surface (Table 10-3). Note that we expressed the properties in units specified under Eq. 10-2 in connection with their definitions in order to avoid unit manipulations.

Analysis (a) The excess temperature in this case is $\Delta T = T_s - T_{\text{sat}} = 108 - 100 = 8^\circ\text{C}$ which is relatively low (less than 30°C). Therefore, nucleate boiling will occur. The heat flux in this case can be determined from the Rohsenow relation to be

$$\begin{aligned} \dot{q}_{\text{nucleate}} &= \mu_l h_{fg} \left[\frac{g(\rho_l - \rho_v)}{\sigma} \right]^{1/2} \left[\frac{C_{pl}(T_s - T_{\text{sat}})}{C_{sf} h_{fg} \text{Pr}_l^n} \right]^3 \\ &= (0.282 \times 10^{-3})(2257 \times 10^3) \left[\frac{9.81 \times (957.9 - 0.6)}{0.0589} \right]^{1/2} \\ &\quad \times \left(\frac{4217(108 - 100)}{0.0130(2257 \times 10^3)1.75} \right)^3 \\ &= 7.20 \times 10^4 \text{ W/m}^2 \end{aligned}$$

The surface area of the bottom of the pan is

$$A = \pi D^2/4 = \pi(0.3 \text{ m})^2/4 = 0.07069 \text{ m}^2$$

Then the rate of heat transfer during nucleate boiling becomes

$$\dot{Q}_{\text{boiling}} = Aq_{\text{nucleate}} = (0.07069 \text{ m}^2)(7.20 \times 10^4 \text{ W/m}^2) = \mathbf{5093 \text{ W}}$$

(b) The rate of evaporation of water is determined from

$$\dot{m}_{\text{evaporation}} = \frac{\dot{Q}_{\text{boiling}}}{h_{fg}} = \frac{5093 \text{ J/s}}{2257 \times 10^3 \text{ J/kg}} = \mathbf{2.26 \times 10^{-3} \text{ kg/s}}$$

That is, water in the pan will boil at a rate of more than 2 grams per second.

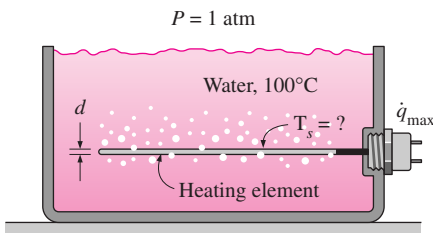


FIGURE 10-16
Schematic for Example 10-2.

EXAMPLE 10-2 Peak Heat Flux in Nucleate Boiling

Water in a tank is to be boiled at sea level by a 1-cm-diameter nickel plated steel heating element equipped with electrical resistance wires inside, as shown in Figure 10-16. Determine the maximum heat flux that can be attained in the nucleate boiling regime and the surface temperature of the heater surface in that case.

SOLUTION Water is boiled at 1 atm pressure on a nickel plated steel surface. The maximum (critical) heat flux and the surface temperature are to be determined.

Assumptions 1 Steady operating conditions exist. 2 Heat losses from the boiler are negligible.

Properties The properties of water at the saturation temperature of 100°C are $\sigma = 0.0589 \text{ N/m}$ (Table 10-1) and, from Table A-9,

$$\begin{aligned} \rho_l &= 957.9 \text{ kg/m}^3 & h_{fg} &= 2257 \times 10^3 \text{ J/kg} \\ \rho_v &= 0.6 \text{ kg/m}^3 & \mu_l &= 0.282 \times 10^{-3} \text{ kg} \cdot \text{m/s} \\ \text{Pr}_l &= 1.75 & C_{pl} &= 4217 \text{ J/kg} \cdot ^\circ\text{C} \end{aligned}$$

Also, $C_{sf} = 0.0060$ and $n = 1.0$ for the boiling of water on a nickel plated surface (Table 10-3). Note that we expressed the properties in units specified under Eqs. 10-2 and 10-3 in connection with their definitions in order to avoid unit manipulations.

Analysis The heating element in this case can be considered to be a short cylinder whose characteristic dimension is its radius. That is, $L = r = 0.005 \text{ m}$. The dimensionless parameter L^* and the constant C_{cr} are determined from Table 10-4 to be

$$L^* = L \left(\frac{g(\rho_l - \rho_v)}{\sigma} \right)^{1/2} = (0.005) \left(\frac{(9.81)(957.8 - 0.6)}{0.0589} \right)^{1/2} = 2.00 > 1.2$$

which corresponds to $C_{cr} = 0.12$.

Then the maximum or critical heat flux is determined from Eq. 10-3 to be

$$\begin{aligned} \dot{q}_{\text{max}} &= C_{cr} h_{fg} [\sigma g \rho_v^2 (\rho_l - \rho_v)]^{1/4} \\ &= 0.12(2257 \times 10^3) [0.0589 \times 9.8 \times (0.6)^2 (957.9 - 0.6)]^{1/4} \\ &= \mathbf{1.02 \times 10^6 \text{ W/m}^2} \end{aligned}$$

The Rohsenow relation, which gives the nucleate boiling heat flux for a specified surface temperature, can also be used to determine the surface temperature when the heat flux is given. Substituting the maximum heat flux into Eq. 10–2 together with other properties gives

$$\dot{q}_{\text{nucleate}} = \mu_l h_{fg} \left[\frac{g(\rho_l - \rho_v)}{\sigma} \right]^{1/2} \left[\frac{C_{pl}(T_s - T_{\text{sat}})^3}{C_{sf} h_{fg} \text{Pr}_l^2} \right]$$

$$1,017,200 = (0.282 \times 10^{-3})(2257 \times 10^3) \left[\frac{9.81(957.9 - 0.6)}{0.0589} \right]^{1/2}$$

$$\left[\frac{4217(T_s - 100)}{0.0130(2257 \times 10^3) 1.75} \right]$$

$$T_s = \mathbf{119^\circ\text{C}}$$

Discussion Note that heat fluxes on the order of 1 MW/m² can be obtained in nucleate boiling with a temperature difference of less than 20°C.

EXAMPLE 10–3 Film Boiling of Water on a Heating Element

Water is boiled at atmospheric pressure by a horizontal polished copper heating element of diameter $D = 5$ mm and emissivity $\varepsilon = 0.05$ immersed in water, as shown in Figure 10–17. If the surface temperature of the heating wire is 350°C, determine the rate of heat transfer from the wire to the water per unit length of the wire.

SOLUTION Water is boiled at 1 atm by a horizontal polished copper heating element. The rate of heat transfer to the water per unit length of the heater is to be determined.

Assumptions 1 Steady operating conditions exist. 2 Heat losses from the boiler are negligible.

Properties The properties of water at the saturation temperature of 100°C are $h_{fg} = 2257 \times 10^3$ J/kg and $\rho_l = 957.9$ kg/m³ (Table A-9). The properties of vapor at the film temperature of $T_f = (T_{\text{sat}} + T_s)/2 = (100 + 350)/2 = 225^\circ\text{C} = 498$ K (which is sufficiently close to 500 K) are, from Table A-16,

$$\begin{aligned} \rho_v &= 0.441 \text{ kg/m}^3 & C_{pv} &= 1977 \text{ J/kg} \cdot ^\circ\text{C} \\ \mu_v &= 1.73 \times 10^{-5} \text{ kg/m} \cdot \text{s} & k_v &= 0.0357 \text{ W/m} \cdot ^\circ\text{C} \end{aligned}$$

Note that we expressed the properties in units that will cancel each other in boiling heat transfer relations. Also note that we used vapor properties at 1 atm pressure from Table A-16 instead of the properties of saturated vapor from Table A-9 at 250°C since the latter are at the saturation pressure of 4.0 MPa.

Analysis The excess temperature in this case is $\Delta T = T_s - T_{\text{sat}} = 350 - 100 = 250^\circ\text{C}$, which is much larger than 30°C for water. Therefore, film boiling will occur. The film boiling heat flux in this case can be determined from Eq. 10–5 to be

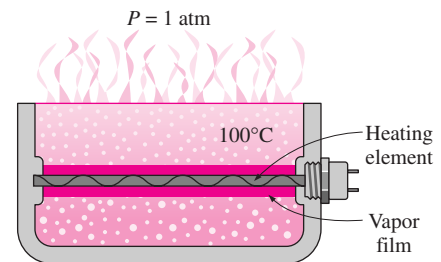


FIGURE 10–17
Schematic for Example 10–3.

$$\begin{aligned} \dot{q}_{\text{film}} &= 0.62 \left[\frac{g k_v^3 \rho_v (\rho_l - \rho_v) [h_{fg} + 0.4 C_{pv} (T_s - T_{\text{sat}})]^{1/4}}{\mu_v D (T_s - T_{\text{sat}})} \right]^{1/4} (T_s - T_{\text{sat}}) \\ &= 0.62 \left[\frac{9.81 (0.0357)^3 (0.441) (957.9 - 0.441)}{[(2257 \times 10^3 + 0.4 \times 1977(250))]} \right]^{1/4} \times 250 \\ &= 5.93 \times 10^4 \text{ W/m}^2 \end{aligned}$$

The radiation heat flux is determined from Eq. 10-6 to be

$$\begin{aligned} \dot{q}_{\text{rad}} &= \epsilon \sigma (T_s^4 - T_{\text{sat}}^4) \\ &= (0.05) (5.67 \times 10^{-8} \text{ W/m}^2 \cdot \text{K}^4) [(250 + 273 \text{ K})^4 - (100 + 273 \text{ K})^4] \\ &= 157 \text{ W/m}^2 \end{aligned}$$

Note that heat transfer by radiation is negligible in this case because of the low emissivity of the surface and the relatively low surface temperature of the heating element. Then the total heat flux becomes (Eq. 10-7)

$$\dot{q}_{\text{total}} = \dot{q}_{\text{film}} + \frac{3}{4} \dot{q}_{\text{rad}} = 5.93 \times 10^4 + \frac{3}{4} \times 157 = 5.94 \times 10^4 \text{ W/m}^2$$

Finally, the rate of heat transfer from the heating element to the water is determined by multiplying the heat flux by the heat transfer surface area,

$$\begin{aligned} \dot{Q}_{\text{total}} &= A \dot{q}_{\text{total}} = (\pi D L) \dot{q}_{\text{total}} \\ &= (\pi \times 0.005 \text{ m} \times 1 \text{ m}) (5.94 \times 10^4 \text{ W/m}^2) \\ &= \mathbf{933 \text{ W}} \end{aligned}$$

Discussion Note that the 5-mm-diameter copper heating element will consume about 1 kW of electric power per unit length in steady operation in the film boiling regime. This energy is transferred to the water through the vapor film that forms around the wire.

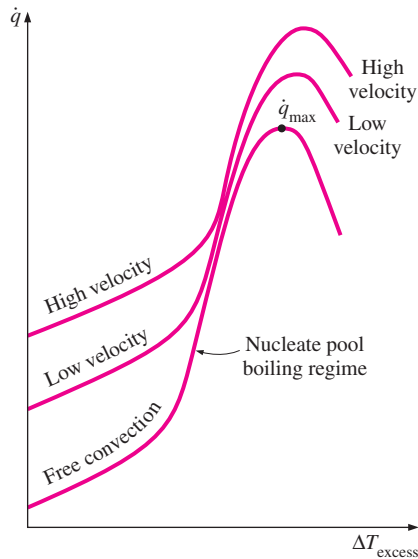


FIGURE 10-18

The effect of forced convection on external flow boiling for different flow velocities.

10-3 ■ FLOW BOILING

The *pool boiling* we considered so far involves a pool of seemingly motionless liquid, with vapor bubbles rising to the top as a result of buoyancy effects. In **flow boiling**, the fluid is forced to move by an external source such as a pump as it undergoes a phase-change process. The boiling in this case exhibits the combined effects of convection and pool boiling. The flow boiling is also classified as either *external* and *internal flow boiling* depending on whether the fluid is forced to flow over a heated surface or inside a heated tube.

External flow boiling over a plate or cylinder is similar to pool boiling, but the added motion increases both the nucleate boiling heat flux and the critical heat flux considerably, as shown in Figure 10-18. Note that the higher the velocity, the higher the nucleate boiling heat flux and the critical heat flux. In experiments with water, critical heat flux values as high as 35 MW/m² have been obtained (compare this to the pool boiling value of 1.3 MW/m² at 1 atm pressure) by increasing the fluid velocity.

Internal flow boiling is much more complicated in nature because there is no free surface for the vapor to escape, and thus both the liquid and the vapor are forced to flow together. The two-phase flow in a tube exhibits different flow boiling regimes, depending on the relative amounts of the liquid and the vapor phases. This complicates the analysis even further.

The different stages encountered in flow boiling in a heated tube are illustrated in Figure 10–19 together with the variation of the heat transfer coefficient along the tube. Initially, the liquid is subcooled and heat transfer to the liquid is by *forced convection*. Then bubbles start forming on the inner surfaces of the tube, and the detached bubbles are drafted into the mainstream. This gives the fluid flow a bubbly appearance, and thus the name *bubbly flow regime*. As the fluid is heated further, the bubbles grow in size and eventually coalesce into slugs of vapor. Up to half of the volume in the tube in this *slug-flow regime* is occupied by vapor. After a while the core of the flow consists of vapor only, and the liquid is confined only in the annular space between the vapor core and the tube walls. This is the *annular-flow regime*, and very high heat transfer coefficients are realized in this regime. As the heating continues, the annular liquid layer gets thinner and thinner, and eventually dry spots start to appear on the inner surfaces of the tube. The appearance of dry spots is accompanied by a sharp decrease in the heat transfer coefficient. This *transition regime* continues until the inner surface of the tube is completely dry. Any liquid at this moment is in the form of droplets suspended in the vapor core, which resembles a mist, and we have a *mist-flow regime* until all the liquid droplets are vaporized. At the end of the mist-flow regime we have saturated vapor, which becomes superheated with any further heat transfer.

Note that the tube contains a liquid before the bubbly flow regime and a vapor after the mist-flow regime. Heat transfer in those two cases can be determined using the appropriate relations for single-phase convection heat transfer. Many correlations are proposed for the determination of heat transfer

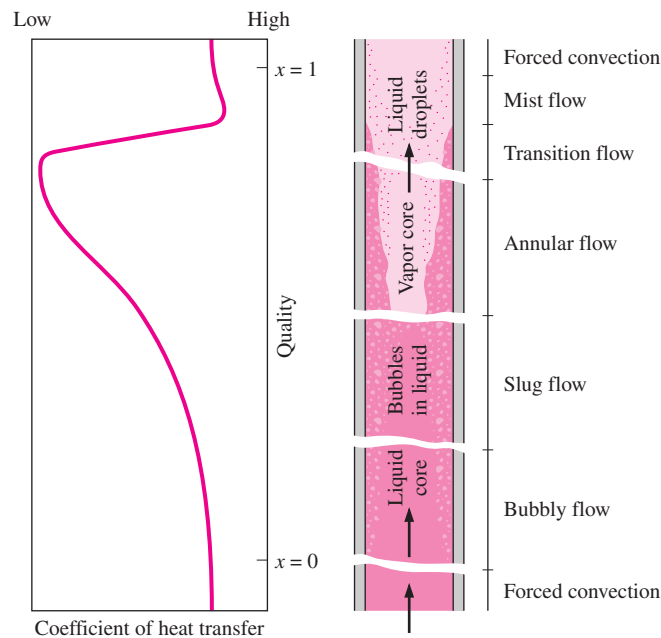
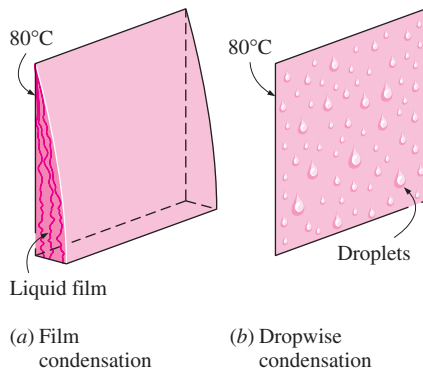


FIGURE 10–19
Different flow regimes encountered in flow boiling in a tube under forced convection.



(a) Film condensation

(b) Dropwise condensation

FIGURE 10-20

When a vapor is exposed to a surface at a temperature below T_{sat} , condensation in the form of a liquid film or individual droplets occurs on the surface.

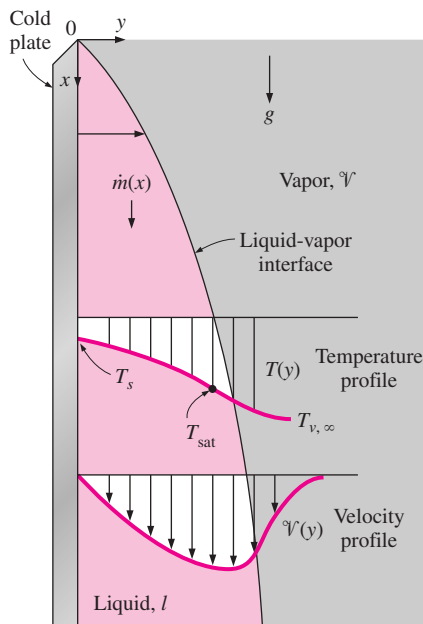


FIGURE 10-21

Film condensation on a vertical plate.

in the two-phase flow (bubbly flow, slug-flow, annular-flow, and mist-flow) cases, but they are beyond the scope of this introductory text. A crude estimate for heat flux in flow boiling can be obtained by simply adding the forced convection and pool boiling heat fluxes.

10-4 ■ CONDENSATION HEAT TRANSFER

Condensation occurs when the temperature of a vapor is reduced *below* its saturation temperature T_{sat} . This is usually done by bringing the vapor into contact with a solid surface whose temperature T_s is *below* the saturation temperature T_{sat} of the vapor. But condensation can also occur on the free surface of a liquid or even in a gas when the temperature of the liquid or the gas to which the vapor is exposed is below T_{sat} . In the latter case, the liquid droplets suspended in the gas form a fog. In this chapter, we will consider condensation on solid surfaces only.

Two distinct forms of condensation are observed: *film condensation* and *dropwise condensation*. In **film condensation**, the condensate wets the surface and forms a liquid film on the surface that slides down under the influence of gravity. The thickness of the liquid film increases in the flow direction as more vapor condenses on the film. This is how condensation normally occurs in practice. In **dropwise condensation**, the condensed vapor forms droplets on the surface instead of a continuous film, and the surface is covered by countless droplets of varying diameters (Fig. 10-20).

In film condensation, the surface is blanketed by a liquid film of increasing thickness, and this “liquid wall” between solid surface and the vapor serves as a *resistance* to heat transfer. The heat of vaporization h_{fg} released as the vapor condenses must pass through this resistance before it can reach the solid surface and be transferred to the medium on the other side. In dropwise condensation, however, the droplets slide down when they reach a certain size, clearing the surface and exposing it to vapor. There is no liquid film in this case to resist heat transfer. As a result, heat transfer rates that are more than 10 times larger than those associated with film condensation can be achieved with dropwise condensation. Therefore, dropwise condensation is the preferred mode of condensation in heat transfer applications, and people have long tried to achieve sustained dropwise condensation by using various vapor additives and surface coatings. These attempts have not been very successful, however, since the dropwise condensation achieved did not last long and converted to film condensation after some time. Therefore, it is common practice to be conservative and assume film condensation in the design of heat transfer equipment.

10-5 ■ FILM CONDENSATION

We now consider film condensation on a vertical plate, as shown in Figure 10-21. The liquid film starts forming at the top of the plate and flows downward under the influence of gravity. The thickness of the film δ *increases* in the flow direction x because of continued condensation at the liquid–vapor interface. Heat in the amount h_{fg} (the latent heat of vaporization) is released during condensation and is *transferred* through the film to the plate surface at temperature T_s . Note that T_s must be below the saturation temperature T_{sat} of the vapor for condensation to occur.

Typical velocity and temperature profiles of the condensate are also given in Figure 10–21. Note that the *velocity* of the condensate at the wall is zero because of the “no-slip” condition and reaches a *maximum* at the liquid–vapor interface. The *temperature* of the condensate is T_{sat} at the interface and decreases gradually to T_s at the wall.

As was the case in forced convection involving a single phase, heat transfer in condensation also depends on whether the condensate flow is *laminar* or *turbulent*. Again the criterion for the flow regime is provided by the Reynolds number, which is defined as

$$\text{Re} = \frac{D_h \rho_l \mathcal{V}_l}{\mu_l} = \frac{4 A_c \rho_l \mathcal{V}_l}{p \mu_l} = \frac{4 \rho_l \mathcal{V}_l \delta}{\mu_l} = \frac{4 \dot{m}}{p \mu_l} \quad (10-8)$$

where

$D_h = 4A_c/p = 4\delta$ = hydraulic diameter of the condensate flow, m

p = wetted perimeter of the condensate, m

$A_c = p\delta$ = wetted perimeter \times film thickness, m^2 , cross-sectional area of the condensate flow at the lowest part of the flow

ρ_l = density of the liquid, kg/m^3

μ_l = viscosity of the liquid, $\text{kg}/\text{m} \cdot \text{s}$

\mathcal{V} = average velocity of the condensate at the lowest part of the flow, m/s

$\dot{m} = \rho_l \mathcal{V}_l A_c$ = mass flow rate of the condensate at the lowest part, kg/s

The evaluation of the hydraulic diameter D_h for some common geometries is illustrated in Figure 10–22. Note that the hydraulic diameter is again defined such that it reduces to the ordinary diameter for flow in a circular tube, as was done in Chapter 8 for internal flow, and it is equivalent to 4 times the thickness of the condensate film at the location where the hydraulic diameter is evaluated. That is, $D_h = 4\delta$.

The latent heat of vaporization h_{fg} is the heat released as a unit mass of vapor condenses, and it normally represents the heat transfer per unit mass of condensate formed during condensation. However, the condensate in an actual

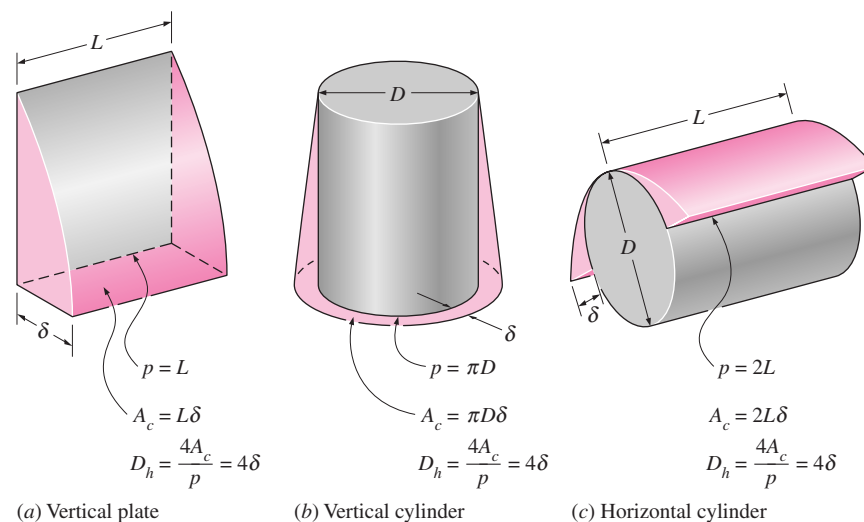


FIGURE 10–22

The wetted perimeter p , the condensate cross-sectional area A_c , and the hydraulic diameter D_h for some common geometries.

condensation process is cooled further to some average temperature between T_{sat} and T_s , releasing *more heat* in the process. Therefore, the actual heat transfer will be larger. Rohsenow showed in 1956 that the cooling of the liquid below the saturation temperature can be accounted for by replacing h_{fg} by the **modified latent heat of vaporization** h_{fg}^* , defined as

$$h_{fg}^* = h_{fg} + 0.68C_{pl}(T_{\text{sat}} - T_s) \quad (10-9a)$$

where C_{pl} is the specific heat of the liquid at the average film temperature.

We can have a similar argument for vapor that enters the condenser as **superheated vapor** at a temperature T_v instead of as saturated vapor. In this case the vapor must be cooled first to T_{sat} before it can condense, and this heat must be transferred to the wall as well. The amount of heat released as a unit mass of superheated vapor at a temperature T_v is cooled to T_{sat} is simply $C_{pv}(T_v - T_{\text{sat}})$, where C_{pv} is the specific heat of the vapor at the average temperature of $(T_v + T_{\text{sat}})/2$. The modified latent heat of vaporization in this case becomes

$$h_{fg}^* = h_{fg} + 0.68C_{pl}(T_{\text{sat}} - T_s) + C_{pv}(T_v - T_{\text{sat}}) \quad (10-9b)$$

With these considerations, the rate of heat transfer can be expressed as

$$\dot{Q}_{\text{conden}} = hA_s(T_{\text{sat}} - T_s) = m\dot{h}_{fg}^* \quad (10-10)$$

where A_s is the heat transfer area (the surface area on which condensation occurs). Solving for \dot{m} from the equation above and substituting it into Eq. 10–8 gives yet another relation for the Reynolds number,

$$\text{Re} = \frac{4\dot{Q}_{\text{conden}}}{\rho\mu_l h_{fg}^*} = \frac{4A_s h(T_{\text{sat}} - T_s)}{\rho\mu_l h_{fg}^*} \quad (10-11)$$

This relation is convenient to use to determine the Reynolds number when the condensation heat transfer coefficient or the rate of heat transfer is known.

The temperature of the liquid film varies from T_{sat} on the liquid–vapor interface to T_s at the wall surface. Therefore, the properties of the liquid should be evaluated at the *film temperature* $T_f = (T_{\text{sat}} + T_s)/2$, which is approximately the *average* temperature of the liquid. The h_{fg} , however, should be evaluated at T_{sat} since it is not affected by the subcooling of the liquid.

Flow Regimes

The Reynolds number for condensation on the outer surfaces of vertical tubes or plates increases in the flow direction due to the increase of the liquid film thickness δ . The flow of liquid film exhibits *different regimes*, depending on the value of the Reynolds number. It is observed that the outer surface of the liquid film remains *smooth* and *wave-free* for about $\text{Re} \leq 30$, as shown in Figure 10–23, and thus the flow is clearly *laminar*. Ripples or waves appear on the free surface of the condensate flow as the Reynolds number increases, and the condensate flow becomes fully *turbulent* at about $\text{Re} \approx 1800$. The condensate flow is called *wavy-laminar* in the range of $450 < \text{Re} < 1800$ and *turbulent* for $\text{Re} > 1800$. However, some disagreement exists about the value of Re at which the flow becomes wavy-laminar or turbulent.

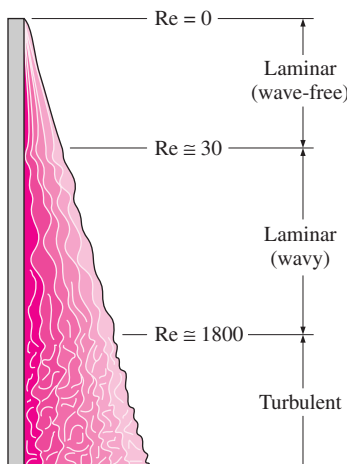


FIGURE 10–23

Flow regimes during film condensation on a vertical plate.

Heat Transfer Correlations for Film Condensation

Below we discuss relations for the average heat transfer coefficient h for the case of *laminar* film condensation for various geometries.

1 Vertical Plates

Consider a vertical plate of height L and width b maintained at a constant temperature T_s that is exposed to vapor at the saturation temperature T_{sat} . The downward direction is taken as the positive x -direction with the origin placed at the top of the plate where condensation initiates, as shown in Figure 10–24. The surface temperature is below the saturation temperature ($T_s < T_{\text{sat}}$) and thus the vapor condenses on the surface. The liquid film flows downward under the influence of gravity. The film thickness δ and thus the mass flow rate of the condensate increases with x as a result of continued condensation on the existing film. Then heat transfer from the vapor to the plate must occur through the film, which offers resistance to heat transfer. Obviously the thicker the film, the larger its thermal resistance and thus the lower the rate of heat transfer.

The analytical relation for the heat transfer coefficient in film condensation on a vertical plate described above was first developed by Nusselt in 1916 under the following simplifying assumptions:

1. Both the plate and the vapor are maintained at *constant temperatures* of T_s and T_{sat} , respectively, and the temperature across the liquid film varies *linearly*.
2. Heat transfer across the liquid film is by pure *conduction* (no convection currents in the liquid film).
3. The velocity of the vapor is low (or zero) so that it exerts *no drag* on the condensate (no viscous shear on the liquid–vapor interface).
4. The flow of the condensate is *laminar* and the properties of the liquid are constant.
5. The acceleration of the condensate layer is negligible.

Then Newton's second law of motion for the volume element shown in Figure 10–24 in the vertical x -direction can be written as

$$\sum F_x = ma_x = 0$$

since the acceleration of the fluid is zero. Noting that the only force acting downward is the weight of the liquid element, and the forces acting upward are the viscous shear (or fluid friction) force at the left and the buoyancy force, the force balance on the volume element becomes

$$\begin{aligned} F_{\text{downward } \downarrow} &= F_{\text{upward } \uparrow} \\ \text{Weight} &= \text{Viscous shear force} + \text{Buoyancy force} \\ \rho_l g(\delta - y)(bdx) &= \mu_l \frac{du}{dy}(bdx) + \rho_v g(\delta - y)(bdx) \end{aligned}$$

Canceling the plate width b and solving for du/dy gives

$$\frac{du}{dy} = \frac{g(\rho_l - \rho_v)(\delta - y)}{\mu_l}$$

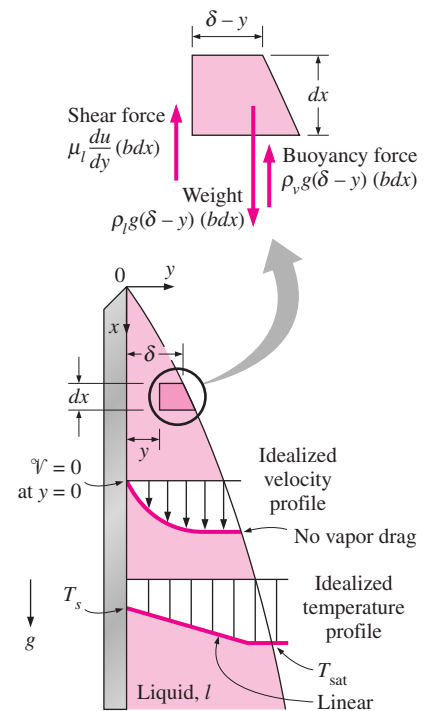


FIGURE 10–24

The volume element of condensate on a vertical plate considered in Nusselt's analysis.

Integrating from $y = 0$ where $u = 0$ (because of the no-slip boundary condition) to $y = y$ where $u = u(y)$ gives

$$u(y) = \frac{g(\rho_l - \rho_v)g}{\mu_l} \left(y\delta - \frac{y^2}{2} \right) \quad (10-12)$$

The mass flow rate of the condensate at a location x , where the boundary layer thickness is δ , is determined from

$$\dot{m}(x) = \int_A \rho_l u(y) dA = \int_{y=0}^{\delta} \rho_l u(y) b dy \quad (10-13)$$

Substituting the $u(y)$ relation from Equation 10–12 into Eq. 10–13 gives

$$\dot{m}(x) = \frac{gb\rho_l(\rho_l - \rho_v)\delta^3}{3\mu_l} \quad (10-14)$$

whose derivative with respect to x is

$$\frac{d\dot{m}}{dx} = \frac{gb\rho_l(\rho_l - \rho_v)\delta^2}{\mu_l} \frac{d\delta}{dx} \quad (10-15)$$

which represents the rate of condensation of vapor over a vertical distance dx . The rate of heat transfer from the vapor to the plate through the liquid film is simply equal to the heat released as the vapor is condensed and is expressed as

$$d\dot{Q} = h_{fg} d\dot{m} = k_l (bdx) \frac{T_{\text{sat}} - T_s}{\delta} \rightarrow \frac{d\dot{m}}{dx} = \frac{k_l b}{h_{fg}} \frac{T_{\text{sat}} - T_s}{\delta} \quad (10-16)$$

Equating Eqs. 10–15 and 10–16 for $d\dot{m}/dx$ to each other and separating the variables give

$$\delta^3 d\delta = \frac{\mu_l k_l (T_{\text{sat}} - T_s)}{g\rho_l(\rho_l - \rho_v)h_{fg}} dx \quad (10-17)$$

Integrating from $x = 0$ where $\delta = 0$ (the top of the plate) to $x = x$ where $\delta = \delta(x)$, the liquid film thickness at any location x is determined to be

$$\delta(x) = \left[\frac{4\mu_l k_l (T_{\text{sat}} - T_s)x}{g\rho_l(\rho_l - \rho_v)h_{fg}} \right]^{1/4} \quad (10-18)$$

The heat transfer rate from the vapor to the plate at a location x can be expressed as

$$\dot{q}_x = h_x(T_{\text{sat}} - T_s) = k_l \frac{T_{\text{sat}} - T_s}{\delta} \rightarrow h_x = \frac{k_l}{\delta(x)} \quad (10-19)$$

Substituting the $\delta(x)$ expression from Eq. 10–18, the local heat transfer coefficient h_x is determined to be

$$h_x = \left[\frac{g\rho_l(\rho_l - \rho_v)h_{fg} k_l^3}{4\mu_l (T_{\text{sat}} - T_s)x} \right]^{1/4} \quad (10-20)$$

The average heat transfer coefficient over the entire plate is determined from its definition by substituting the h_x relation and performing the integration. It gives

$$h = h_{\text{ave}} = \frac{1}{L} \int_0^L h_x dx = \frac{4}{3} h_{x=L} = 0.943 \left[\frac{g\rho_l(\rho_l - \rho_v)h_{fg}k_l^3}{\mu_l(T_{\text{sat}} - T_s)L} \right]^{1/4} \quad (10-21)$$

Equation 10–21, which is obtained with the simplifying assumptions stated earlier, provides good insight on the functional dependence of the condensation heat transfer coefficient. However, it is observed to underpredict heat transfer because it does not take into account the effects of the nonlinear temperature profile in the liquid film and the cooling of the liquid below the saturation temperature. Both of these effects can be accounted for by replacing h_{fg} by h_{fg}^* given by Eq. 10–9. With this modification, the *average heat transfer coefficient* for laminar film condensation over a vertical flat plate of height L is determined to be

$$h_{\text{vert}} = 0.943 \left[\frac{g\rho_l(\rho_l - \rho_v)h_{fg}^*k_l^3}{\mu_l(T_{\text{sat}} - T_s)L} \right]^{1/4} \quad (\text{W/m}^2 \cdot ^\circ\text{C}), 0 < \text{Re} < 30 \quad (10-22)$$

where

g = gravitational acceleration, m/s^2

ρ_l, ρ_v = densities of the liquid and vapor, respectively, kg/m^3

μ_l = viscosity of the liquid, $\text{kg/m} \cdot \text{s}$

$h_{fg}^* = h_{fg} + 0.68C_{pl}(T_{\text{sat}} - T_s)$ = modified latent heat of vaporization, J/kg

k_l = thermal conductivity of the liquid, $\text{W/m} \cdot ^\circ\text{C}$

L = height of the vertical plate, m

T_s = surface temperature of the plate, $^\circ\text{C}$

T_{sat} = saturation temperature of the condensing fluid, $^\circ\text{C}$

At a given temperature, $\rho_v \ll \rho_l$ and thus $\rho_l - \rho_v \approx \rho_l$ except near the critical point of the substance. Using this approximation and substituting Eqs. 10–14 and 10–18 at $x = L$ into Eq. 10–8 by noting that $\delta_{x=L} = \frac{k_l}{h_{x=L}}$ and $h_{\text{vert}} = \frac{4}{3} h_{x=L}$ (Eqs. 10–19 and 10–21) give

$$\text{Re} \cong \frac{4g\rho_l(\rho_l - \rho_v)\delta^3}{3\mu_l^2} = \frac{4g\rho_l^2 \left(\frac{k_l}{h_{x=L}}\right)^3}{3\mu_l^2} = \frac{4g}{3\nu_l^2} \left(\frac{k_l}{3h_{\text{vert}}/4}\right)^3 \quad (10-23)$$

Then the heat transfer coefficient h_{vert} in terms of Re becomes

$$h_{\text{vert}} \cong 1.47k_l \text{Re}^{-1/3} \left(\frac{g}{\nu_l^2}\right)^{1/3}, \quad \begin{array}{l} 0 < \text{Re} < 30 \\ \rho_v \ll \rho_l \end{array} \quad (10-24)$$

The results obtained from the theoretical relations above are in excellent agreement with the experimental results. It can be shown easily that using property values in Eqs. 10–22 and 10–24 in the *specified units* gives the condensation heat transfer coefficient in $\text{W/m}^2 \cdot ^\circ\text{C}$, thus saving one from having

$$\begin{aligned}
 h_{\text{vert}} &= \left(\frac{\frac{\text{m}}{\text{s}^2} \frac{\text{kg}}{\text{m}^3} \frac{\text{kg}}{\text{m}^3} \frac{\text{J}}{\text{m} \cdot \text{kg}} \left(\frac{\text{W}}{\text{m} \cdot \text{C}} \right)^3}{\frac{\text{kg}}{\text{m} \cdot \text{s}} \cdot \text{C} \cdot \text{m}} \right)^{1/4} \\
 &= \left[\frac{\text{m}}{\text{s}} \frac{1}{\text{m}^6} \frac{\text{W}^3}{\text{m}^3} \frac{\text{J}}{\text{C}^3} \right]^{1/4} \\
 &= \left(\frac{\text{W}^4}{\text{m}^8 \cdot \text{C}^4} \right)^{1/4} \\
 &= \text{W}/\text{m}^2 \cdot \text{C}
 \end{aligned}$$

FIGURE 10-25

Equation 10-22 gives the condensation heat transfer coefficient in $\text{W}/\text{m}^2 \cdot \text{C}$ when the quantities are expressed in the units specified in their descriptions.

to go through tedious unit manipulations each time (Fig. 10-25). This is also true for the equations below. All properties of the *liquid* are to be evaluated at the film temperature $T_f = (T_{\text{sat}} + T_s)/2$. The h_{fg} and ρ_v are to be evaluated at the saturation temperature T_{sat} .

Wavy Laminar Flow on Vertical Plates

At Reynolds numbers greater than about 30, it is observed that waves form at the liquid–vapor interface although the flow in liquid film remains laminar. The flow in this case is said to be *wavy laminar*. The waves at the liquid–vapor interface tend to increase heat transfer. But the waves also complicate the analysis and make it very difficult to obtain analytical solutions. Therefore, we have to rely on experimental studies. The increase in heat transfer due to the wave effect is, on average, about 20 percent, but it can exceed 50 percent. The exact amount of enhancement depends on the Reynolds number. Based on his experimental studies, Kutateladze (1963, Ref. 15) recommended the following relation for the average heat transfer coefficient in wavy laminar condensate flow for $\rho_v \ll \rho_l$ and $30 < \text{Re} < 1800$,

$$h_{\text{vert, wavy}} = \frac{\text{Re } k_l}{1.08 \text{Re}^{1.22} - 5.2} \left(\frac{g}{\nu_l^2} \right)^{1/3}, \quad \begin{array}{l} 30 < \text{Re} < 1800 \\ \rho_v \ll \rho_l \end{array} \quad (10-25)$$

A simpler alternative to the relation above proposed by Kutateladze (1963, Ref. 15) is

$$h_{\text{vert, wavy}} = 0.8 \text{Re}^{0.11} h_{\text{vert (smooth)}} \quad (10-26)$$

which relates the heat transfer coefficient in wavy laminar flow to that in wave-free laminar flow. McAdams (1954, Ref. 2) went even further and suggested accounting for the increase in heat transfer in the wavy region by simply increasing the heat transfer coefficient determined from Eq. 10-22 for the laminar case by 20 percent. Holman (1990) suggested using Eq. 10-22 for the wavy region also, with the understanding that this is a conservative approach that provides a safety margin in thermal design. In this book we will use Eq. 10-25.

A relation for the Reynolds number in the wavy laminar region can be determined by substituting the h relation in Eq. 10-25 into the Re relation in Eq. 10-11 and simplifying. It yields

$$\text{Re}_{\text{vert, wavy}} = \left[4.81 + \frac{3.70 L k_l (T_{\text{sat}} - T_s)}{\mu_l h_{fg}^*} \left(\frac{g}{\nu_l^2} \right)^{1/3} \right]^{0.820}, \quad \rho_v \ll \rho_l \quad (10-27)$$

Turbulent Flow on Vertical Plates

At a Reynolds number of about 1800, the condensate flow becomes turbulent. Several empirical relations of varying degrees of complexity are proposed for the heat transfer coefficient for turbulent flow. Again assuming $\rho_v \ll \rho_l$ for simplicity, Labuntsov (1957, Ref. 17) proposed the following relation for the turbulent flow of condensate on *vertical plates*:

$$h_{\text{vert, turbulent}} = \frac{\text{Re } k_l}{8750 + 58 \text{Pr}^{-0.5} (\text{Re}^{0.75} - 253)} \left(\frac{g}{\nu_l^2} \right)^{1/3}, \quad \begin{array}{l} \text{Re} > 1800 \\ \rho_v \ll \rho_l \end{array} \quad (10-28)$$

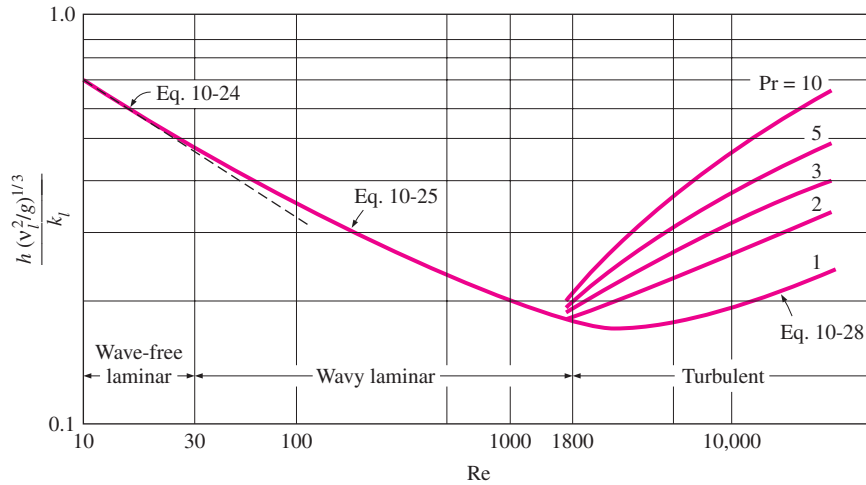


FIGURE 10-26 Nondimensionalized heat transfer coefficients for the wave-free laminar, wavy laminar, and turbulent flow of condensate on vertical plates.

The physical properties of the condensate are again to be evaluated at the film temperature $T_f = (T_{sat} + T_s)/2$. The Re relation in this case is obtained by substituting the h relation above into the Re relation in Eq. 10-11, which gives

$$Re_{\text{vert, turbulent}} = \left[\frac{0.0690 L k_f Pr^{0.5} (T_{sat} - T_s) \left(\frac{g}{v_f^2}\right)^{1/3} - 151 Pr^{0.5} + 253}{\mu_l h_{fg}^*} \right]^{4/3} \quad (10-29)$$

Nondimensionalized heat transfer coefficients for the wave-free laminar, wavy laminar, and turbulent flow of condensate on vertical plates are plotted in Figure 10-26.

2 Inclined Plates

Equation 10-12 was developed for vertical plates, but it can also be used for laminar film condensation on the upper surfaces of plates that are *inclined* by an angle θ from the *vertical*, by replacing g in that equation by $g \cos \theta$ (Fig. 10-27). This approximation gives satisfactory results especially for $\theta \leq 60^\circ$. Note that the condensation heat transfer coefficients on vertical and inclined plates are related to each other by

$$h_{\text{inclined}} = h_{\text{vert}} (\cos \theta)^{1/4} \quad (\text{laminar}) \quad (10-30)$$

Equation 10-30 is developed for laminar flow of condensate, but it can also be used for wavy laminar flows as an approximation.

3 Vertical Tubes

Equation 10-22 for vertical plates can also be used to calculate the average heat transfer coefficient for laminar film condensation on the outer surfaces of vertical tubes provided that the tube diameter is large relative to the thickness of the liquid film.

4 Horizontal Tubes and Spheres

Nusselt's analysis of film condensation on vertical plates can also be extended to horizontal tubes and spheres. The average heat transfer coefficient for film condensation on the outer surfaces of a *horizontal tube* is determined to be

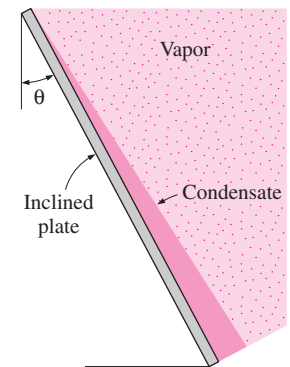
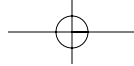


FIGURE 10-27 Film condensation on an inclined plate.



$$h_{\text{horiz}} = 0.729 \left[\frac{g\rho_l(\rho_l - \rho_v) h_{fg}^* k_l^3}{\mu_l(T_{\text{sat}} - T_s)D} \right]^{1/4} \quad (\text{W/m}^2 \cdot ^\circ\text{C}) \quad (10-31)$$

where D is the diameter of the horizontal tube. Equation 10–31 can easily be modified for a *sphere* by replacing the constant 0.729 by 0.815.

A comparison of the heat transfer coefficient relations for a vertical tube of height L and a horizontal tube of diameter D yields

$$\frac{h_{\text{vert}}}{h_{\text{horiz}}} = 1.29 \left(\frac{D}{L} \right)^{1/4} \quad (10-32)$$

Setting $h_{\text{vertical}} = h_{\text{horizontal}}$ gives $L = 1.29^4 D = 2.77D$, which implies that for a tube whose length is 2.77 times its diameter, the average heat transfer coefficient for laminar film condensation will be the *same* whether the tube is positioned horizontally or vertically. For $L > 2.77D$, the heat transfer coefficient will be higher in the horizontal position. Considering that the length of a tube in any practical application is several times its diameter, it is common practice to place the tubes in a condenser *horizontally* to *maximize* the condensation heat transfer coefficient on the outer surfaces of the tubes.

5 Horizontal Tube Banks

Horizontal tubes stacked on top of each other as shown in Figure 10–28 are commonly used in condenser design. The average thickness of the liquid film at the lower tubes is much larger as a result of condensate falling on top of them from the tubes directly above. Therefore, the average heat transfer coefficient at the lower tubes in such arrangements is smaller. Assuming the condensate from the tubes above to the ones below drain smoothly, the average film condensation heat transfer coefficient for all tubes in a vertical tier can be expressed as

$$h_{\text{horiz}, N \text{ tubes}} = 0.729 \left[\frac{g\rho_l(\rho_l - \rho_v) h_{fg}^* k_l^3}{\mu_l(T_{\text{sat}} - T_s)ND} \right]^{1/4} = \frac{1}{N^{1/4}} h_{\text{horiz}, 1 \text{ tube}} \quad (10-33)$$

Note that Eq. 10–33 can be obtained from the heat transfer coefficient relation for a horizontal tube by replacing D in that relation by ND . This relation does not account for the increase in heat transfer due to the ripple formation and turbulence caused during drainage, and thus generally yields conservative results.

Effect of Vapor Velocity

In the analysis above we assumed the vapor velocity to be small and thus the vapor drag exerted on the liquid film to be negligible, which is usually the case. However, when the vapor velocity is high, the vapor will “pull” the liquid at the interface along since the vapor velocity at the interface must drop to the value of the liquid velocity. If the vapor flows downward (i.e., in the same direction as the liquid), this additional force will increase the average velocity of the liquid and thus decrease the film thickness. This, in turn, will decrease the thermal resistance of the liquid film and thus increase heat transfer. Upward vapor flow has the opposite effects: the vapor exerts a force on the

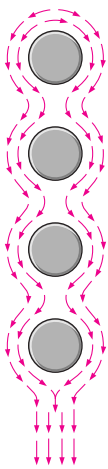
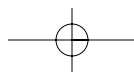
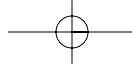


FIGURE 10–28
Film condensation on a vertical tier of horizontal tubes.





liquid in the opposite direction to flow, thickens the liquid film, and thus decreases heat transfer. Condensation in the presence of high vapor flow is studied [e.g., Shekrladze and Gomelauri (1966), Ref. 23] and heat transfer relations are obtained, but a detailed analysis of this topic is beyond the scope of this introductory text.

The Presence of Noncondensable Gases in Condensers

Most condensers used in steam power plants operate at pressures well below the atmospheric pressure (usually under 0.1 atm) to maximize cycle thermal efficiency, and operation at such low pressures raises the possibility of air (a noncondensable gas) leaking into the condensers. Experimental studies show that the presence of noncondensable gases in the vapor has a detrimental effect on condensation heat transfer. Even small amounts of a noncondensable gas in the vapor cause significant drops in heat transfer coefficient during condensation. For example, the presence of less than 1 percent (by mass) of air in steam can reduce the condensation heat transfer coefficient by more than half. Therefore, it is common practice to periodically vent out the noncondensable gases that accumulate in the condensers to ensure proper operation.

The drastic reduction in the condensation heat transfer coefficient in the presence of a noncondensable gas can be explained as follows: When the vapor mixed with a noncondensable gas condenses, only the noncondensable gas remains in the vicinity of the surface (Fig. 10–29). This gas layer acts as a *barrier* between the vapor and the surface, and makes it difficult for the vapor to reach the surface. The vapor now must diffuse through the noncondensable gas first before reaching the surface, and this reduces the effectiveness of the condensation process.

Experimental studies show that heat transfer in the presence of a noncondensable gas strongly depends on the nature of the vapor flow and the flow velocity. As you would expect, a *high flow velocity* is more likely to remove the stagnant noncondensable gas from the vicinity of the surface, and thus *improve* heat transfer.

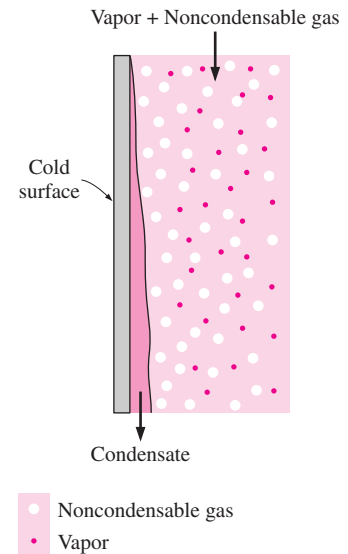


FIGURE 10–29

The presence of a noncondensable gas in a vapor prevents the vapor molecules from reaching the cold surface easily, and thus impedes condensation heat transfer.

EXAMPLE 10–4 Condensation of Steam on a Vertical Plate

Saturated steam at atmospheric pressure condenses on a 2-m-high and 3-m-wide vertical plate that is maintained at 80°C by circulating cooling water through the other side (Fig. 10–30). Determine (a) the rate of heat transfer by condensation to the plate and (b) the rate at which the condensate drips off the plate at the bottom.

SOLUTION Saturated steam at 1 atm condenses on a vertical plate. The rates of heat transfer and condensation are to be determined.

Assumptions 1 Steady operating conditions exist. 2 The plate is isothermal. 3 The condensate flow is wavy-laminar over the entire plate (will be verified). 4 The density of vapor is much smaller than the density of liquid, $\rho_v \ll \rho_l$.

Properties The properties of water at the saturation temperature of 100°C are $h_{fg} = 2257 \times 10^3 \text{ J/kg}$ and $\rho_v = 0.60 \text{ kg/m}^3$. The properties of liquid water at the film temperature of $T_f = (T_{\text{sat}} + T_s)/2 = (100 + 80)/2 = 90^\circ\text{C}$ are (Table A-9)

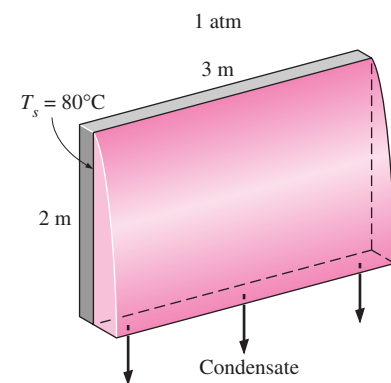


FIGURE 10–30

Schematic for Example 10–4.

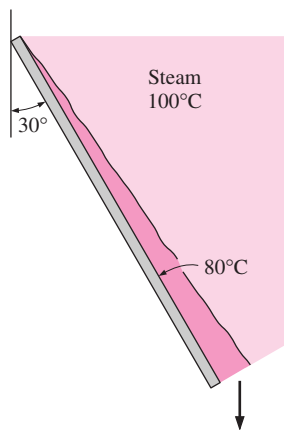


FIGURE 10-31
Schematic for Example 10-5.

$$\begin{aligned}\rho_l &= 965.3 \text{ kg/m}^3 & C_{pl} &= 4206 \text{ J/kg} \cdot ^\circ\text{C} \\ \mu_l &= 0.315 \times 10^{-3} \text{ kg/m} \cdot \text{s} & k_l &= 0.675 \text{ W/m} \cdot ^\circ\text{C} \\ \nu_l &= \mu_l/\rho_l = 0.326 \times 10^{-6} \text{ m}^2/\text{s}\end{aligned}$$

Analysis (a) The modified latent heat of vaporization is

$$\begin{aligned}h_{fg}^* &= h_{fg} + 0.68C_{pl}(T_{\text{sat}} - T_s) \\ &= 2257 \times 10^3 \text{ J/kg} + 0.68 \times (4206 \text{ J/kg} \cdot ^\circ\text{C})(100 - 80)^\circ\text{C} \\ &= 2314 \times 10^3 \text{ J/kg}\end{aligned}$$

For wavy-laminar flow, the Reynolds number is determined from Eq. 10-27 to be

$$\begin{aligned}\text{Re} &= \text{Re}_{\text{vertical, wavy}} = \left[4.81 + \frac{3.70 L k_l (T_{\text{sat}} - T_s) \left(\frac{g}{\nu_l^2}\right)^{1/3}}{\mu_l h_{fg}^*} \right]^{0.820} \\ &= \left[4.81 + \frac{3.70(3 \text{ m})(0.675 \text{ W/m} \cdot ^\circ\text{C})(100 - 90)^\circ\text{C}}{(0.315 \times 10^{-3} \text{ kg/m} \cdot \text{s})(2314 \times 10^3 \text{ J/kg})} \right. \\ &\quad \left. \times \left(\frac{9.81 \text{ m/s}^2}{(0.326 \times 10^{-6} \text{ m}^2/\text{s})^2} \right)^{1/3} \right]^{0.82} \\ &= 1287\end{aligned}$$

which is between 30 and 1800, and thus our assumption of wavy laminar flow is verified. Then the condensation heat transfer coefficient is determined from Eq. 10-25 to be

$$\begin{aligned}h &= h_{\text{vertical, wavy}} = \frac{\text{Re} k_l}{1.08 \text{Re}^{1.22} - 5.2} \left(\frac{g}{\nu_l^2}\right)^{1/3} \\ &= \frac{1287 \times (0.675 \text{ W/m} \cdot ^\circ\text{C})}{1.08(1287)^{1.22} - 5.2} \left(\frac{9.81 \text{ m/s}^2}{(0.326 \times 10^{-6} \text{ m}^2/\text{s})^2}\right)^{1/3} = 5848 \text{ W/m}^2 \cdot ^\circ\text{C}\end{aligned}$$

The heat transfer surface area of the plate is $A_s = W \times L = (3 \text{ m})(2 \text{ m}) = 6 \text{ m}^2$. Then the rate of heat transfer during this condensation process becomes

$$\dot{Q} = hA_s(T_{\text{sat}} - T_s) = (5848 \text{ W/m}^2 \cdot ^\circ\text{C})(6 \text{ m}^2)(100 - 80)^\circ\text{C} = \mathbf{7.02 \times 10^5 \text{ W}}$$

(b) The rate of condensation of steam is determined from

$$\dot{m}_{\text{condensation}} = \frac{\dot{Q}}{h_{fg}^*} = \frac{7.02 \times 10^5 \text{ J/s}}{2314 \times 10^3 \text{ J/kg}} = \mathbf{0.303 \text{ kg/s}}$$

That is, steam will condense on the surface at a rate of 303 grams per second.

EXAMPLE 10-5 Condensation of Steam on a Tilted Plate

What would your answer be to the preceding example problem if the plate were tilted 30° from the vertical, as shown in Figure 10-31?

SOLUTION (a) The heat transfer coefficient in this case can be determined from the vertical plate relation by replacing g by $g \cos \theta$. But we will use Eq. 10–30 instead since we already know the value for the vertical plate from the preceding example:

$$h = h_{\text{inclined}} = h_{\text{vert}} (\cos \theta)^{1/4} = (5848 \text{ W/m}^2 \cdot ^\circ\text{C})(\cos 30^\circ)^{1/4} = 5641 \text{ W/m}^2 \cdot ^\circ\text{C}$$

The heat transfer surface area of the plate is still 6 m^2 . Then the rate of condensation heat transfer in the tilted plate case becomes

$$\dot{Q} = hA_s(T_{\text{sat}} - T_s) = (5641 \text{ W/m}^2 \cdot ^\circ\text{C})(6 \text{ m}^2)(100 - 80)^\circ\text{C} = \mathbf{6.77 \times 10^5 \text{ W}}$$

(b) The rate of condensation of steam is again determined from

$$\dot{m}_{\text{condensation}} = \frac{\dot{Q}}{h_{fg}^*} = \frac{6.77 \times 10^5 \text{ J/s}}{2314 \times 10^3 \text{ J/kg}} = \mathbf{0.293 \text{ kg/s}}$$

Discussion Note that the rate of condensation decreased by about 3.6 percent when the plate is tilted.

EXAMPLE 10–6 Condensation of Steam on Horizontal Tubes

The condenser of a steam power plant operates at a pressure of 7.38 kPa. Steam at this pressure condenses on the outer surfaces of horizontal pipes through which cooling water circulates. The outer diameter of the pipes is 3 cm, and the outer surfaces of the pipes are maintained at 30°C (Fig. 10–32). Determine (a) the rate of heat transfer to the cooling water circulating in the pipes and (b) the rate of condensation of steam per unit length of a horizontal pipe.

SOLUTION Saturated steam at a pressure of 7.38 kPa (Table A-9) condenses on a horizontal tube at 30°C . The rates of heat transfer and condensation are to be determined.

Assumptions 1 Steady operating conditions exist. 2 The tube is isothermal.

Properties The properties of water at the saturation temperature of 40°C corresponding to 7.38 kPa are $h_{fg} = 2407 \times 10^3 \text{ J/kg}$ and $\rho_v = 0.05 \text{ kg/m}^3$. The properties of liquid water at the film temperature of $T_f = (T_{\text{sat}} + T_s)/2 = (40 + 30)/2 = 35^\circ\text{C}$ are (Table A-9)

$$\begin{aligned} \rho_l &= 994 \text{ kg/m}^3 & C_{pl} &= 4178 \text{ J/kg} \cdot ^\circ\text{C} \\ \mu_l &= 0.720 \times 10^{-3} \text{ kg/m} \cdot \text{s} & k_l &= 0.623 \text{ W/m} \cdot ^\circ\text{C} \end{aligned}$$

Analysis (a) The modified latent heat of vaporization is

$$\begin{aligned} h_{fg}^* &= h_{fg} + 0.68C_{pl}(T_{\text{sat}} - T_s) \\ &= 2407 \times 10^3 \text{ J/kg} + 0.68 \times (4178 \text{ J/kg} \cdot ^\circ\text{C})(40 - 30)^\circ\text{C} \\ &= 2435 \times 10^3 \text{ J/kg} \end{aligned}$$

Noting that $\rho_v \ll \rho_l$ (since $0.05 \ll 994$), the heat transfer coefficient for condensation on a single horizontal tube is determined from Eq. 10–31 to be

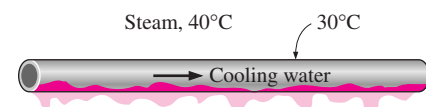


FIGURE 10–32
Schematic for Example 10–6.

$$\begin{aligned}
 h &= h_{\text{horizontal}} = 0.729 \left[\frac{g\rho_l(\rho_l - \rho_v) h_{fg}^* k_l^3}{\mu(T_{\text{sat}} - T_s) D} \right]^{1/4} \cong 0.729 \left[\frac{g\rho_l^2 h_{fg}^* k_l^3}{\mu_1 (T_{\text{sat}} - T_s) D} \right]^{1/4} \\
 &= 0.729 \left[\frac{(9.81 \text{ m/s}^2)(994 \text{ kg/m}^3)^2 (2435 \times 10^3 \text{ J/kg})(0.623 \text{ W/m} \cdot \text{ }^\circ\text{C})^3}{(0.720 \times 10^{-3} \text{ kg/m} \cdot \text{s})(40 - 30)^\circ\text{C}(0.03 \text{ m})} \right]^{1/4} \\
 &= 9292 \text{ W/m}^2 \cdot \text{ }^\circ\text{C}
 \end{aligned}$$

The heat transfer surface area of the pipe per unit of its length is $A_s = \pi DL = \pi(0.03 \text{ m})(1 \text{ m}) = 0.09425 \text{ m}^2$. Then the rate of heat transfer during this condensation process becomes

$$\dot{Q} = hA_s(T_{\text{sat}} - T_s) = (9292 \text{ W/m}^2 \cdot \text{ }^\circ\text{C})(0.09425 \text{ m}^2)(40 - 30)^\circ\text{C} = \mathbf{8758 \text{ W}}$$

(b) The rate of condensation of steam is

$$\dot{m}_{\text{condensation}} = \frac{\dot{Q}}{h_{fg}^*} = \frac{8758 \text{ J/s}}{2435 \times 10^3 \text{ J/kg}} = \mathbf{0.00360 \text{ kg/s}}$$

Therefore, steam will condense on the horizontal tube at a rate of 3.6 g/s or 12.9 kg/h per meter of its length.

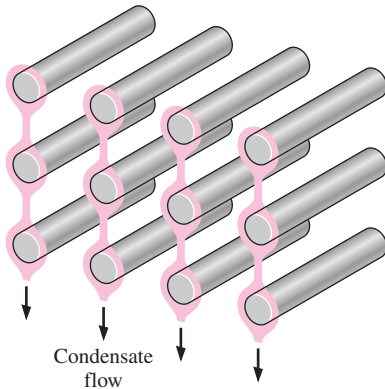


FIGURE 10-33
Schematic for Example 10-7.

EXAMPLE 10-7 Condensation of Steam on Horizontal Tube Banks

Repeat the preceding example problem for the case of 12 horizontal tubes arranged in a rectangular array of 3 tubes high and 4 tubes wide, as shown in Figure 10-33.

SOLUTION (a) Condensation heat transfer on a tube is not influenced by the presence of other tubes in its neighborhood unless the condensate from other tubes drips on it. In our case, the horizontal tubes are arranged in four vertical tiers, each tier consisting of 3 tubes. The average heat transfer coefficient for a vertical tier of N horizontal tubes is related to the one for a single horizontal tube by Eq. 10-33 and is determined to be

$$h_{\text{horiz, } N \text{ tubes}} = \frac{1}{N^{1/4}} h_{\text{horiz, 1 tube}} = \frac{1}{3^{1/4}} (9292 \text{ W/m}^2 \cdot \text{ }^\circ\text{C}) = 7060 \text{ W/m}^2 \cdot \text{ }^\circ\text{C}$$

Each vertical tier consists of 3 tubes, and thus the heat transfer coefficient determined above is valid for each of the four tiers. In other words, this value can be taken to be the average heat transfer coefficient for all 12 tubes.

The surface area for all 12 tubes per unit length of the tubes is

$$A_s = N_{\text{total}} \pi DL = 12\pi(0.03 \text{ m})(1 \text{ m}) = 1.1310 \text{ m}^2$$

Then the rate of heat transfer during this condensation process becomes

$$\dot{Q} = hA_s(T_{\text{sat}} - T_s) = (7060 \text{ W/m}^2 \cdot \text{ }^\circ\text{C})(1.131 \text{ m}^2)(40 - 30)^\circ\text{C} = \mathbf{79,850 \text{ W}}$$

(b) The rate of condensation of steam is again determined from

$$\dot{m}_{\text{condensation}} = \frac{\dot{Q}}{h_{fg}^*} = \frac{79,850 \text{ J/s}}{2435 \times 10^3 \text{ J/kg}} = 0.0328 \text{ kg/s}$$

Therefore, steam will condense on the horizontal pipes at a rate of 32.8 g/s per meter length of the tubes.

10-6 ■ FILM CONDENSATION INSIDE HORIZONTAL TUBES

So far we have discussed film condensation on the *outer surfaces* of tubes and other geometries, which is characterized by negligible vapor velocity and the unrestricted flow of the condensate. Most condensation processes encountered in refrigeration and air-conditioning applications, however, involve condensation on the *inner surfaces* of horizontal or vertical tubes. Heat transfer analysis of condensation inside tubes is complicated by the fact that it is strongly influenced by the vapor velocity and the rate of liquid accumulation on the walls of the tubes (Fig. 10-34).

For *low vapor velocities*, Chato recommends this expression for condensation

$$h_{\text{internal}} = 0.555 \left[\frac{g \rho_l (\rho_l - \rho_v) k_l^3}{\mu_l (T_{\text{sat}} - T_s)} \left(h_{fg} + \frac{3}{8} C_{pl} (T_{\text{sat}} - T_s) \right) \right]^{1/4} \quad (10-34)$$

for

$$\text{Re}_{\text{vapor}} = \left(\frac{\rho_v V_v D}{\mu_v} \right)_{\text{inlet}} < 35,000 \quad (10-35)$$

where the Reynolds number of the vapor is to be evaluated at the tube *inlet* conditions using the internal tube diameter as the characteristic length. Heat transfer coefficient correlations for higher vapor velocities are given by Rohsenow.

10-7 ■ DROPWISE CONDENSATION

Dropwise condensation, characterized by countless droplets of varying diameters on the condensing surface instead of a continuous liquid film, is one of the most effective mechanisms of heat transfer, and extremely large heat transfer coefficients can be achieved with this mechanism (Fig. 10-35).

In dropwise condensation, the small droplets that form at the nucleation sites on the surface grow as a result of continued condensation, coalesce into large droplets, and slide down when they reach a certain size, clearing the surface and exposing it to vapor. There is no liquid film in this case to resist heat transfer. As a result, with dropwise condensation, heat transfer coefficients can be achieved that are more than 10 times larger than those associated with film condensation. Large heat transfer coefficients enable designers to achieve a specified heat transfer rate with a smaller surface area, and thus a smaller (and

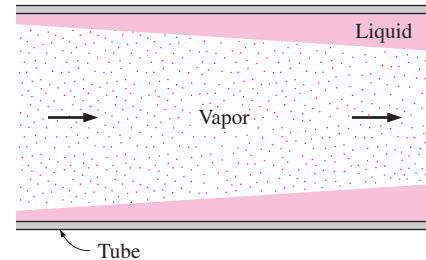


FIGURE 10-34
Condensate flow in a horizontal tube with large vapor velocities.



FIGURE 10-35
Dropwise condensation of steam on a vertical surface (from Hampson and Özişik, Ref. 11).

less expensive) condenser. Therefore, dropwise condensation is the preferred mode of condensation in heat transfer applications.

The challenge in dropwise condensation is not to achieve it, but rather, to *sustain* it for prolonged periods of time. Dropwise condensation is achieved by *adding* a promoting chemical into the vapor, *treating* the surface with a promoter chemical, or *coating* the surface with a polymer such as teflon or a noble metal such as gold, silver, rhodium, palladium, or platinum. The *promoters* used include various waxes and fatty acids such as oleic, stearic, and linoic acids. They lose their effectiveness after a while, however, because of fouling, oxidation, and the removal of the promoter from the surface. It is possible to sustain dropwise condensation for over a year by the combined effects of surface coating and periodic injection of the promoter into the vapor. However, any gain in heat transfer must be weighed against the cost associated with sustaining dropwise condensation.

Dropwise condensation has been studied experimentally for a number of surface–fluid combinations. Of these, the studies on the condensation of steam on copper surfaces has attracted the most attention because of their widespread use in steam power plants. P. Griffith (1983) recommends these simple correlations for dropwise condensation of *steam on copper surfaces*:

$$h_{\text{dropwise}} = \begin{cases} 51,104 + 2044T_{\text{sat}}, & 22^{\circ}\text{C} < T_{\text{sat}} < 100^{\circ}\text{C} \\ 255,310 & T_{\text{sat}} > 100^{\circ}\text{C} \end{cases} \quad \begin{matrix} (10-36) \\ (10-37) \end{matrix}$$

where T_{sat} is in $^{\circ}\text{C}$ and the heat transfer coefficient h_{dropwise} is in $\text{W}/\text{m}^2 \cdot ^{\circ}\text{C}$.

The very high heat transfer coefficients achievable with dropwise condensation are of little significance if the material of the condensing surface is not a good conductor like copper or if the thermal resistance on the other side of the surface is too large. In steady operation, heat transfer from one medium to another depends on the sum of the thermal resistances on the path of heat flow, and a large thermal resistance may overshadow all others and dominate the heat transfer process. In such cases, improving the accuracy of a small resistance (such as one due to condensation or boiling) makes hardly any difference in overall heat transfer calculations.

TOPIC OF SPECIAL INTEREST*

Heat Pipes

A **heat pipe** is a simple device with no moving parts that can transfer large quantities of heat over fairly large distances essentially at a constant temperature without requiring any power input. A heat pipe is basically a sealed slender tube containing a wick structure lined on the inner surface and a small amount of fluid such as water at the saturated state, as shown in Figure 10–36. It is composed of three sections: the *evaporator* section at one end, where heat is absorbed and the fluid is vaporized; a *condenser* section at the other end, where the vapor is condensed and heat is rejected; and the *adiabatic* section in between, where the vapor and the liquid phases of the fluid flow in opposite directions through the core and the wick,

*This section can be skipped without a loss in continuity.

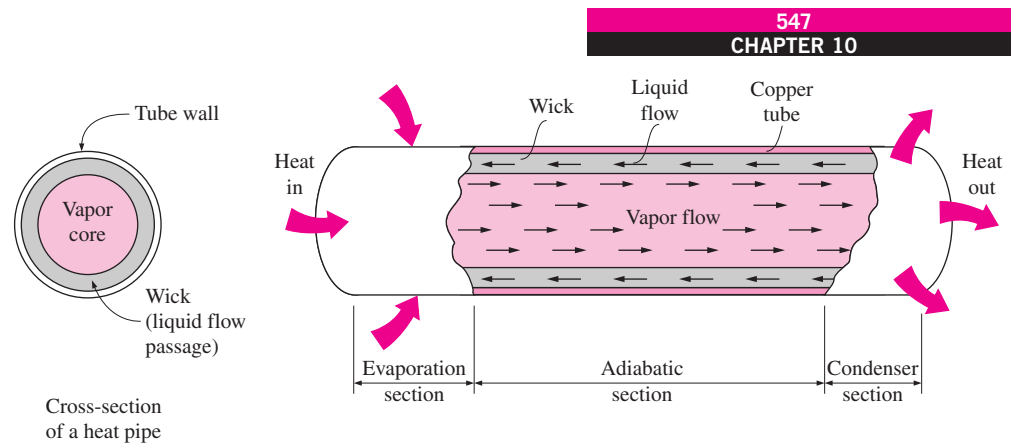


FIGURE 10-36
Schematic and operation of a heat pipe.

respectively, to complete the cycle with no significant heat transfer between the fluid and the surrounding medium.

The *type of fluid* and the *operating pressure* inside the heat pipe depend on the *operating temperature* of the heat pipe. For example, the critical- and triple-point temperatures of water are 0.01°C and 374.1°C , respectively. Therefore, water can undergo a liquid-to-vapor or vapor-to-liquid phase change process in this temperature range only, and thus it will not be a suitable fluid for applications involving temperatures beyond this range. Furthermore, water will undergo a phase-change process at a specified temperature only if its pressure equals the saturation pressure at that temperature. For example, if a heat pipe with water as the working fluid is designed to remove heat at 70°C , the pressure inside the heat pipe must be maintained at 31.2 kPa, which is the boiling pressure of water at this temperature. Note that this value is well below the atmospheric pressure of 101 kPa, and thus the heat pipe will operate in a vacuum environment in this case. If the pressure inside is maintained at the local atmospheric pressure instead, heat transfer would result in an increase in the temperature of the water instead of evaporation.

Although water is a suitable fluid to use in the moderate temperature range encountered in electronic equipment, several other fluids can be used in the construction of heat pipes to enable them to be used in cryogenic as well as high-temperature applications. The suitable temperature ranges for some common heat pipe fluids are given in Table 10-5. Note that the overall temperature range extends from almost absolute zero for cryogenic fluids such as helium to over 1600°C for liquid metals such as lithium. The ultimate temperature limits for a fluid are the *triple-* and *critical-point* temperatures. However, a narrower temperature range is used in practice to avoid the extreme pressures and low heats of vaporization that occur near the critical point. Other desirable characteristics of the candidate fluids are having a high surface tension to enhance the capillary effect and being compatible with the wick material, as well as being readily available, chemically stable, nontoxic, and inexpensive.

The concept of heat pipe was originally conceived by R. S. Gaugler of the General Motors Corporation, who filed a patent application for it in

TABLE 10-5

Suitable temperature ranges for some fluids used in heat pipes

Fluid	Temperature Range, $^{\circ}\text{C}$
Helium	-271 to -268
Hydrogen	-259 to -240
Neon	-248 to -230
Nitrogen	-210 to -150
Methane	-182 to -82
Ammonia	-78 to -130
Water	5 to 230
Mercury	200 to 500
Cesium	400 to 1000
Sodium	500 to 1200
Lithium	850 to 1600

1942. However, it did not receive much attention until 1962, when it was suggested for use in space applications. Since then, heat pipes have found a wide range of applications, including the cooling of electronic equipment.

The Operation of a Heat Pipe

The operation of a heat pipe is based on the following physical principles:

- At a specified pressure, a liquid will vaporize or a vapor will condense at a certain temperature, called the *saturation temperature*. Thus, fixing the pressure inside a heat pipe fixes the temperature at which phase change will occur.
- At a specified pressure or temperature, the amount of heat *absorbed* as a unit mass of liquid vaporizes is equal to the amount of heat *rejected* as that vapor condenses.
- The capillary pressure developed in a wick will move a liquid in the wick even *against* the gravitational field as a result of the capillary effect.
- A fluid in a channel flows in the direction of *decreasing pressure*.

Initially, the *wick* of the heat pipe is saturated with liquid and the *core section* is filled with vapor. When the evaporator end of the heat pipe is brought into contact with a hot surface or is placed into a hot environment, heat will transfer into the heat pipe. Being at a saturated state, the liquid in the evaporator end of the heat pipe will *vaporize* as a result of this heat transfer, causing the vapor pressure there to rise. This resulting pressure difference drives the vapor through the core of the heat pipe from the evaporator toward the condenser section. The condenser end of the heat pipe is in a cooler environment, and thus its surface is slightly cooler. The vapor that comes into contact with this cooler surface *condenses*, releasing the heat a vaporization, which is rejected to the surrounding medium. The liquid then returns to the evaporator end of the heat pipe through the wick as a result of *capillary action* in the wick, completing the cycle. As a result, heat is absorbed at one end of the heat pipe and is rejected at the other end, with the fluid inside serving as a transport medium for heat.

The boiling and condensation processes are associated with extremely high heat transfer coefficients, and thus it is natural to expect the heat pipe to be a very effective heat transfer device, since its operation is based on alternative boiling and condensation of the working fluid. Indeed, heat pipes have effective conductivities *several hundred times* that of copper or silver. That is, replacing a copper bar between two mediums at different temperatures by a heat pipe of equal size can increase the rate of heat transfer between those two mediums by several hundred times. A simple heat pipe with water as the working fluid has an effective thermal conductivity of the order of $100,000 \text{ W/m} \cdot ^\circ\text{C}$ compared with about $400 \text{ W/m} \cdot ^\circ\text{C}$ for copper. For a heat pipe, it is not unusual to have an effective conductivity of $400,000 \text{ W/m} \cdot ^\circ\text{C}$, which is 1000 times that of copper. A 15-cm-long, 0.6-cm-diameter horizontal cylindrical heat pipe with water inside, for example, can transfer heat at a rate of 300 W. Therefore, heat pipes are preferred in some critical applications, despite their high initial cost.

There is a small pressure difference between the evaporator and condenser ends, and thus a small temperature difference between the two ends of the heat pipe. This temperature difference is usually between 1°C and 5°C.

The Construction of a Heat Pipe

The wick of a heat pipe provides the means for the return of the liquid to the evaporator. Therefore, the structure of the wick has a strong effect on the performance of a heat pipe, and the design and construction of the wick are the most critical aspects of the manufacturing process.

The wicks are often made of porous ceramic or woven stainless wire mesh. They can also be made together with the tube by extruding axial grooves along its inner surface, but this approach presents manufacturing difficulties.

The performance of a wick depends on its structure. The characteristics of a wick can be changed by changing the *size* and the *number* of the pores per unit volume and the *continuity* of the passageway. Liquid motion in the wick depends on the dynamic balance between two opposing effects: the *capillary pressure*, which creates the suction effect to draw the liquid, and the *internal resistance to flow* as a result of friction between the mesh surfaces and the liquid. A small pore size increases the capillary action, since the capillary pressure is inversely proportional to the effective capillary radius of the mesh. But decreasing the pore size and thus the capillary radius also increases the friction force opposing the motion. Therefore, the core size of the mesh should be reduced so long as the increase in capillary force is greater than the increase in the friction force.

Note that the *optimum pore size* will be different for different fluids and different orientations of the heat pipe. An improperly designed wick will result in an inadequate liquid supply and eventual failure of the heat pipe.

Capillary action permits the heat pipe to operate in any orientation in a gravity field. However, the performance of a heat pipe will be best when the capillary and gravity forces act in the same direction (evaporator end down) and will be worst when these two forces act in opposite directions (evaporator end up). Gravity does not affect the capillary force when the heat pipe is in the horizontal position. The heat removal capacity of a horizontal heat pipe can be *doubled* by installing it vertically with evaporator end down so that gravity helps the capillary action. In the opposite case, vertical orientation with evaporator end up, the performance declines considerably relative the horizontal case since the capillary force in this case must work against the gravity force.

Most heat pipes are cylindrical in shape. However, they can be manufactured in a variety of shapes involving 90° bends, S-turns, or spirals. They can also be made as a flat layer with a thickness of about 0.3 cm. Flat heat pipes are very suitable for cooling high-power-output (say, 50 W or greater) PCBs. In this case, flat heat pipes are attached directly to the back surface of the PCB, and they absorb and transfer the heat to the edges. Cooling fins are usually attached to the condenser end of the heat pipe to improve its effectiveness and to eliminate a bottleneck in the path of heat flow from the components to the environment when the ultimate heat sink is the ambient air.

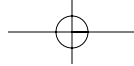
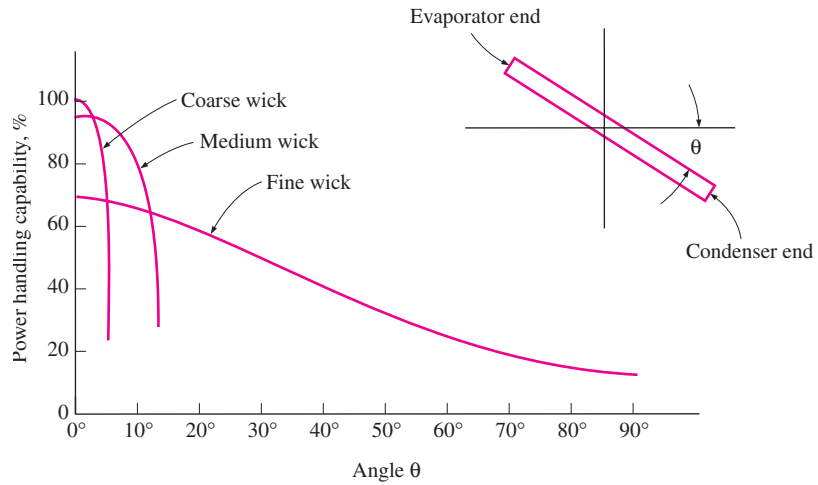


FIGURE 10-37
Variation of the heat removal capacity of a heat pipe with tilt angle from the horizontal when the liquid flows in the wick against gravity (from Steinberg, Ref. 18).



The decline in the performance of a 122-cm-long water heat pipe with the tilt angle from the horizontal is shown in Figure 10-37 for heat pipes with coarse, medium, and fine wicks. Note that for the horizontal case, the heat pipe with a coarse wick performs best, but the performance drops off sharply as the evaporator end is raised from the horizontal. The heat pipe with a fine wick does not perform as well in the horizontal position but maintains its level of performance greatly at tilted positions. It is clear from this figure that heat pipes that work against gravity must be equipped with *fine* wicks. The heat removal capacities of various heat pipes are given in Table 10-6.

TABLE 10-6

Typical heat removal capacity of various heat pipes

Outside Diameter, cm (in.)	Length, cm (in.)	Heat Removal Rate, W
0.64($\frac{1}{4}$)	15.2(6)	300
	30.5(12)	175
	45.7(18)	150
0.95($\frac{3}{8}$)	15.2(6)	500
	30.5(12)	375
	45.7(18)	350
1.27($\frac{1}{2}$)	15.2(6)	700
	30.5(12)	575
	45.7(18)	550

A major concern about the performance of a heat pipe is degradation with time. Some heat pipes have failed within just a few months after they are put into operation. The major cause of degradation appears to be *contamination* that occurs during the sealing of the ends of the heat pipe tube and affects the vapor pressure. This form of contamination has been minimized by electron beam welding in clean rooms. Contamination of the wick prior to installation in the tube is another cause of degradation. Cleanliness of the wick is essential for its reliable operation for a long time. Heat pipes usually undergo extensive testing and quality control process before they are put into actual use.

An important consideration in the design of heat pipes is the compatibility of the materials used for the tube, wick, and fluid. Otherwise, reaction between the incompatible materials produces noncondensable gases, which degrade the performance of the heat pipe. For example, the reaction between stainless steel and water in some early heat pipes generated hydrogen gas, which destroyed the heat pipe.

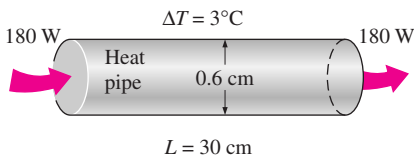
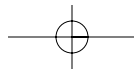


FIGURE 10-38
Schematic for Example 10-8.

EXAMPLE 10-8 Replacing a Heat Pipe by a Copper Rod

A 30-cm-long cylindrical heat pipe having a diameter of 0.6 cm is dissipating heat at a rate of 180 W, with a temperature difference of 3°C across the heat pipe, as shown in Figure 10-38. If we were to use a 30-cm-long copper rod in-



stead to remove heat at the same rate, determine the diameter and the mass of the copper rod that needs to be installed.

SOLUTION A cylindrical heat pipe dissipates heat at a specified rate. The diameter and mass of a copper rod that can conduct heat at the same rate are to be determined.

Assumptions Steady operating conditions exist.

Properties The properties of copper at room temperature are $\rho = 8950 \text{ kg/m}^3$ and $k = 386 \text{ W/m} \cdot ^\circ\text{C}$.

Analysis The rate of heat transfer \dot{Q} through the copper rod can be expressed as

$$\dot{Q} = kA \frac{\Delta T}{L}$$

where k is the thermal conductivity, L is the length, and ΔT is the temperature difference across the copper bar. Solving for the cross-sectional area A and substituting the specified values gives

$$A = \frac{L}{k\Delta T} \dot{Q} = \frac{0.3 \text{ m}}{(386 \text{ W/m} \cdot ^\circ\text{C})(3^\circ\text{C})} (180 \text{ W}) = 0.04663 \text{ m}^2 = 466.3 \text{ cm}^2$$

Then the diameter and the mass of the copper rod become

$$A = \frac{1}{4}\pi D^2 \longrightarrow D = \sqrt{4A/\pi} = \sqrt{4(466.3 \text{ cm}^2)/\pi} = \mathbf{24.4 \text{ cm}}$$

$$m = \rho V = \rho AL = (8950 \text{ kg/m}^3)(0.04663 \text{ m}^2)(0.3 \text{ m}) = \mathbf{125.2 \text{ kg}}$$

Therefore, the diameter of the copper rod needs to be almost 25 times that of the heat pipe to transfer heat at the same rate. Also, the rod would have a mass of 125.2 kg, which is impossible for an average person to lift.

SUMMARY

Boiling occurs when a liquid is in contact with a surface maintained at a temperature T_s sufficiently above the saturation temperature T_{sat} of the liquid. Boiling is classified as *pool boiling* or *flow boiling* depending on the presence of bulk fluid motion. Boiling is called *pool boiling* in the absence of bulk fluid flow and *flow boiling* (or *forced convection boiling*) in its presence. Pool and flow boiling are further classified as *subcooled boiling* and *saturated boiling* depending on the bulk liquid temperature. Boiling is said to be *subcooled* (or *local*) when the temperature of the main body of the liquid is below the saturation temperature T_{sat} and *saturated* (or *bulk*) when the temperature of the liquid is equal to T_{sat} . Boiling exhibits different regimes depending on the value of the excess temperature ΔT_{excess} . Four different boiling regimes are observed: natural convection boiling, nucleate boiling, transition boiling, and film boiling. These regimes are illustrated on the *boiling curve*.

The rate of evaporation and the rate of heat transfer in nucleate boiling increase with increasing ΔT_{excess} and reach a maximum at some point. The heat flux at this point is called the *critical* (or *maximum*) *heat flux*, \dot{q}_{max} . The rate of heat transfer in nucleate pool boiling is determined from

$$\dot{q}_{\text{nucleate}} = \mu_l h_{fg} \left[\frac{g(\rho_l - \rho_v)}{\sigma} \right]^{1/2} \left[\frac{C_{pl}(T_s - T_{\text{sat}})}{C_{sf} h_{fg} \text{Pr}_l^n} \right]^3$$

The *maximum* (or *critical*) *heat flux* in nucleate pool boiling is determined from

$$\dot{q}_{\text{max}} = C_{\text{cr}} h_{fg} [\sigma g \rho_v^2 (\rho_l - \rho_v)]^{1/4}$$

where the value of the constant C_{cr} is about 0.15. The minimum heat flux is given by

$$\dot{q}_{\min} = 0.09 \rho_v h_{fg} \left[\frac{\sigma g (\rho_l - \rho_v)}{(\rho_l - \rho_v)^2} \right]^{1/4}$$

The heat flux for stable *film boiling* on the outside of a *horizontal cylinder* or *sphere* of diameter D is given by

$$\dot{q}_{\text{film}} = C_{\text{film}} \left[\frac{g k_v^3 \rho_v (\rho_l - \rho_v) [h_{fg} + 0.4 C_{pv} (T_s - T_{\text{sat}})]}{\rho_v D (T_s - T_{\text{sat}})} \right]^{1/4} \times (T_s - T_{\text{sat}})$$

where the constant $C_{\text{film}} = 0.62$ for horizontal cylinders and 0.67 for spheres, and k_v is the thermal conductivity of the vapor. The *vapor* properties are to be evaluated at the *film temperature* $T_f = (T_{\text{sat}} + T_s)/2$, which is the *average temperature* of the vapor film. The liquid properties and h_{fg} are to be evaluated at the saturation temperature at the specified pressure.

Two distinct forms of condensation are observed in nature: film condensation and dropwise condensation. In *film condensation*, the condensate wets the surface and forms a liquid film on the surface that slides down under the influence of gravity. In *dropwise condensation*, the condensed vapor forms countless droplets of varying diameters on the surface instead of a continuous film.

The Reynolds number for the condensate flow is defined as

$$\text{Re} = \frac{D_h \rho_l \bar{V}_l}{\mu_l} = \frac{4 A \rho_l \bar{V}_l}{p \mu_l} = \frac{4 \dot{m}}{p \mu_l}$$

and

$$\text{Re} = \frac{4 \dot{Q}_{\text{conden}}}{p \mu_l h_{fg}^*} = \frac{4 A_s h (T_{\text{sat}} - T_s)}{p \mu_l h_{fg}^*}$$

where h_{fg}^* is the *modified latent heat of vaporization*, defined as

$$h_{fg}^* = h_{fg} + 0.68 C_{pl} (T_{\text{sat}} - T_s)$$

and represents heat transfer during condensation per unit mass of condensate. Here C_{pl} is the specific heat of the liquid in $\text{J/kg} \cdot ^\circ\text{C}$.

Using some simplifying assumptions, the *average heat transfer coefficient* for film condensation on a vertical plate of height L is determined to be

$$h_{\text{vert}} = 0.943 \left[\frac{g \rho_l (\rho_l - \rho_v) h_{fg}^* k_l^3}{\mu_l (T_s - T_{\text{sat}}) L} \right]^{1/4} \quad (\text{W/m}^2 \cdot ^\circ\text{C})$$

All properties of the *liquid* are to be evaluated at the film temperature $T_f = (T_{\text{sat}} + T_s)/2$. The h_{fg} and ρ_v are to be evaluated at T_{sat} . Condensate flow is *smooth* and *wave-free laminar* for about $\text{Re} \leq 30$, *wavy-laminar* in the range of $30 < \text{Re} < 1800$,

and fully *turbulent* for $\text{Re} > 1800$. Heat transfer coefficients in the wavy-laminar and turbulent flow regions are determined from

$$h_{\text{vert, wavy}} = \frac{\text{Re } k_l}{1.08 \text{Re}^{1.22} - 5.2} \left(\frac{g}{v_l^2} \right)^{1/3}, \quad 30 < \text{Re} < 1800 \\ \rho_v \ll \rho_l$$

$$h_{\text{vert, turbulent}} = \frac{\text{Re } k_l}{8750 + 58 \text{Pr}^{-0.5} (\text{Re}^{0.75} - 253)} \left(\frac{g}{v_l^2} \right)^{1/3}, \quad \text{Re} > 1800 \\ \rho_v \ll \rho_l$$

Equations for vertical plates can also be used for laminar film condensation on the upper surfaces of the plates that are inclined by an angle θ from the vertical, by replacing g in that equation by $g \cos \theta$. Vertical plate equations can also be used to calculate the average heat transfer coefficient for laminar film condensation on the outer surfaces of vertical tubes provided that the tube diameter is large relative to the thickness of the liquid film.

The average heat transfer coefficient for film condensation on the outer surfaces of a *horizontal tube* is determined to be

$$h_{\text{horiz}} = 0.729 \left[\frac{g \rho_l (\rho_l - \rho_v) h_{fg}^* k_l^3}{\mu_l (T_s - T_{\text{sat}}) D} \right]^{1/4} \quad (\text{W/m}^2 \cdot ^\circ\text{C})$$

where D is the diameter of the horizontal tube. This relation can easily be modified for a *sphere* by replacing the constant 0.729 by 0.815. It can also be used for N *horizontal tubes* stacked on top of each other by replacing D in the denominator by ND .

For low vapor velocities, film condensation heat transfer *inside horizontal tubes* can be determined from

$$h_{\text{internal}} = 0.555 \left[\frac{g \rho_l (\rho_l - \rho_v) k_l^3}{\mu_l (T_{\text{sat}} - T_s)} \left(h_{fg} + \frac{3}{8} C_{pl} (T_{\text{sat}} - T_s) \right) \right]^{1/4}$$

and

$$\text{Re}_{\text{vapor}} = \left(\frac{\rho_v \bar{V}_v D}{\mu_v} \right)_{\text{inlet}} < 35,000$$

where the Reynolds number of the vapor is to be evaluated at the tube inlet conditions using the internal tube diameter as the characteristic length. Finally, the heat transfer coefficient for *dropwise condensation* of steam on copper surfaces is given by

$$h_{\text{dropwise}} = \begin{cases} 51,104 + 2044 T_{\text{sat}}, & 22^\circ\text{C} < T_{\text{sat}} < 100^\circ\text{C} \\ 255,310, & T_{\text{sat}} > 100^\circ\text{C} \end{cases}$$

where T_{sat} is in $^\circ\text{C}$ and the heat transfer coefficient h_{dropwise} is in $\text{W/m}^2 \cdot ^\circ\text{C}$.

REFERENCES AND SUGGESTED READING



1. N. Arai, T. Fukushima, A. Arai, T. Nakajima, K. Fujie, and Y. Nakayama. "Heat Transfer Tubes Enhancing Boiling and Condensation in Heat Exchangers of a Refrigeration Machine." *ASHRAE Journal* 83 (1977), p. 58.
2. P. J. Berensen. "Film Boiling Heat Transfer for a Horizontal Surface." *Journal of Heat Transfer* 83 (1961), pp. 351–358.
3. P. J. Berensen. "Experiments in Pool Boiling Heat Transfer." *International Journal of Heat Mass Transfer* 5 (1962), pp. 985–999.
4. L. A. Bromley. "Heat Transfer in Stable Film Boiling." *Chemical Engineering Prog.* 46 (1950), pp. 221–227.
5. J. C. Chato. "Laminar Condensation inside Horizontal and Inclined Tubes." *ASHRAE Journal* 4 (1962), p. 52.
6. S. W. Chi. *Heat Theory and Practice*. Washington, D.C.: Hemisphere, 1976.
7. M. T. Cichelli and C. F. Bonilla. "Heat Transfer to Liquids Boiling under Pressure." *Transactions of AIChE* 41 (1945), pp. 755–787.
8. R. A. Colclaser, D. A. Neaman, and C. F. Hawkins. *Electronic Circuit Analysis*. New York: John Wiley & Sons, 1984.
9. J. W. Dally. *Packaging of Electronic Systems*. New York: McGraw-Hill, 1960.
10. P. Griffith. "Dropwise Condensation." In *Heat Exchanger Design Handbook*, ed. E. U. Schlunder, Vol 2, Ch. 2.6.5. New York: Hemisphere, 1983.
11. H. Hampson and N. Özişik. "An Investigation into the Condensation of Steam." *Proceedings of the Institute of Mechanical Engineers*, London 1B (1952), pp. 282–294.
12. J. P. Holman. *Heat Transfer*. 8th ed. New York: McGraw-Hill, 1997.
13. F. P. Incropera and D. P. DeWitt. *Introduction to Heat Transfer*. 4th ed. New York: John Wiley & Sons, 2002.
14. J. J. Jasper. "The Surface Tension of Pure Liquid Compounds." *Journal of Physical and Chemical Reference Data* 1, No. 4 (1972), pp. 841–1009.
15. R. Kemp. "The Heat Pipe—A New Tune on an Old Pipe." *Electronics and Power* (August 9, 1973), p. 326.
16. S. S. Kutateladze. *Fundamentals of Heat Transfer*. New York: Academic Press, 1963.
17. S. S. Kutateladze. "On the Transition to Film Boiling under Natural Convection." *Kotloturbostroenie* 3 (1948), p. 48.
18. D. A. Labuntsov. "Heat Transfer in Film Condensation of Pure Steam on Vertical Surfaces and Horizontal Tubes." *Teploenergetika* 4 (1957), pp. 72–80.
19. J. H. Lienhard and V. K. Dhir. "Extended Hydrodynamic Theory of the Peak and Minimum Pool Boiling Heat Fluxes." NASA Report, NASA-CR-2270, July 1973.
20. J. H. Lienhard and V. K. Dhir. "Hydrodynamic Prediction of Peak Pool Boiling Heat Fluxes from Finite Bodies." *Journal of Heat Transfer* 95 (1973), pp. 152–158.
21. W. H. McAdams. *Heat Transmission*. 3rd ed. New York: McGraw-Hill, 1954.
22. W. M. Rohsenow. "A Method of Correlating Heat Transfer Data for Surface Boiling of Liquids." *ASME Transactions* 74 (1952), pp. 969–975.
23. D. S. Steinberg. *Cooling Techniques for Electronic Equipment*. New York: John Wiley & Sons, 1980.
24. W. M. Rohsenow. "Film Condensation." In *Handbook of Heat Transfer*, ed. W. M. Rohsenow and J. P. Hartnett, Ch. 12A. New York: McGraw-Hill, 1973.
25. I. G. Shekrladze, I. G. Gomelauri, and V. I. Gomelauri. "Theoretical Study of Laminar Film Condensation of Flowing Vapor." *International Journal of Heat Mass Transfer* 9 (1966), pp. 591–592.
26. N. V. Suryanarayana. *Engineering Heat Transfer*. St. Paul, MN: West Publishing, 1995.
27. J. W. Westwater and J. G. Santangelo. *Industrial Engineering Chemistry* 47 (1955), p. 1605.
28. N. Zuber. "On the Stability of Boiling Heat Transfer." *ASME Transactions* 80 (1958), pp. 711–720.

PROBLEMS*

Boiling Heat Transfer

10–1C What is boiling? What mechanisms are responsible for the very high heat transfer coefficients in nucleate boiling?

10–2C Does the amount of heat absorbed as 1 kg of saturated liquid water boils at 100°C have to be equal to the amount of heat released as 1 kg of saturated water vapor condenses at 100°C?

*Problems designated by a "C" are concept questions, and students are encouraged to answer them all. Problems designated by an "E" are in English units, and the SI users can ignore them. Problems with an EES-CD icon  are solved using EES, and complete solutions together with parametric studies are included on the enclosed CD. Problems with a computer-EES icon  are comprehensive in nature, and are intended to be solved with a computer, preferably using the EES software that accompanies this text.

10-3C What is the difference between evaporation and boiling?

10-4C What is the difference between pool boiling and flow boiling?

10-5C What is the difference between subcooled and saturated boiling?

10-6C Draw the boiling curve and identify the different boiling regimes. Also, explain the characteristics of each regime.

10-7C How does film boiling differ from nucleate boiling? Is the boiling heat flux necessarily higher in the stable film boiling regime than it is in the nucleate boiling regime?

10-8C Draw the boiling curve and identify the burnout point on the curve. Explain how burnout is caused. Why is the burnout point avoided in the design of boilers?

10-9C Discuss some methods of enhancing pool boiling heat transfer permanently.

10-10C Name the different boiling regimes in the order they occur in a vertical tube during flow boiling.

10-11 Water is to be boiled at atmospheric pressure in a mechanically polished steel pan placed on top of a heating unit. The inner surface of the bottom of the pan is maintained at 110°C . If the diameter of the bottom of the pan is 25 cm, determine (a) the rate of heat transfer to the water and (b) the rate of evaporation.

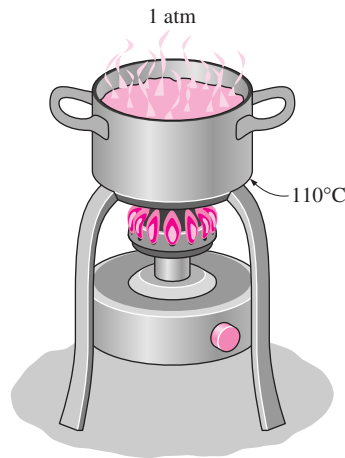



FIGURE P10-11

10-12 Water is to be boiled at atmospheric pressure on a 3-cm-diameter mechanically polished steel heater. Determine the maximum heat flux that can be attained in the nucleate boiling regime and the surface temperature of the heater surface in that case.

10-13  Reconsider Problem 10-12. Using EES (or other) software, investigate the effect of local atmospheric pressure on the maximum heat flux and the temperature difference $T_s - T_{\text{sat}}$. Let the atmospheric pressure vary

from 70 kPa and 101.3 kPa. Plot the maximum heat flux and the temperature difference as a function of the atmospheric pressure, and discuss the results.

10-14E Water is boiled at atmospheric pressure by a horizontal polished copper heating element of diameter $D = 0.5$ in. and emissivity $\varepsilon = 0.08$ immersed in water. If the surface temperature of the heating element is 788°F , determine the rate of heat transfer to the water per unit length of the heating element.

Answer: 2465 Btu/h

10-15E Repeat Problem 10-14E for a heating element temperature of 988°F .

10-16 Water is to be boiled at sea level in a 30-cm-diameter mechanically polished AISI 304 stainless steel pan placed on top of a 3-kW electric burner. If 60 percent of the heat generated by the burner is transferred to the water during boiling, determine the temperature of the inner surface of the bottom of the pan. Also, determine the temperature difference between the inner and outer surfaces of the bottom of the pan if it is 6 mm thick.

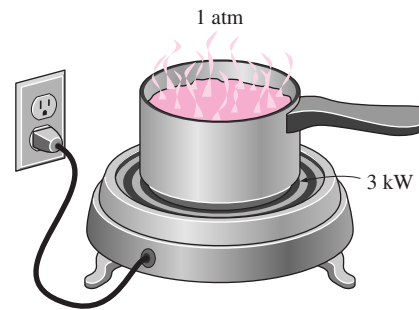


FIGURE P10-16

10-17 Repeat Problem 10-16 for a location at an elevation of 1500 m where the atmospheric pressure is 84.5 kPa and thus the boiling temperature of water is 95°C .

Answers: 100.9°C , 10.3°C

10-18 Water is boiled at sea level in a coffee maker equipped with a 20-cm long 0.4-cm-diameter immersion-type electric

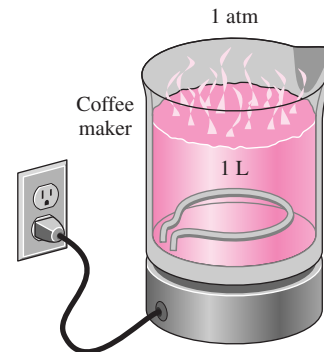


FIGURE P10-18


heating element made of mechanically polished stainless steel. The coffee maker initially contains 1 L of water at 18°C. Once boiling starts, it is observed that half of the water in the coffee maker evaporates in 25 min. Determine the power rating of the electric heating element immersed in water and the surface temperature of the heating element. Also determine how long it will take for this heater to raise the temperature of 1 L of cold water from 18°C to the boiling temperature.

10-19 Repeat Problem 10-18 for a copper heating element.

10-20 A 65-cm-long, 2-cm-diameter brass heating element is to be used to boil water at 120°C. If the surface temperature of the heating element is not to exceed 125°C, determine the highest rate of steam production in the boiler, in kg/h.

Answer: 19.4 kg/h

10-21 To understand the burnout phenomenon, boiling experiments are conducted in water at atmospheric pressure using an electrically heated 30-cm-long, 3-mm-diameter nickel-plated horizontal wire. Determine (a) the critical heat flux and (b) the increase in the temperature of the wire as the operating point jumps from the nucleate boiling to the film boiling regime at the critical heat flux. Take the emissivity of the wire to be 0.5.

10-22  Reconsider Problem 10-21. Using EES (or other) software, investigate the effects of the local atmospheric pressure and the emissivity of the wire on the critical heat flux and the temperature rise of wire. Let the atmospheric pressure vary from 70 kPa and 101.3 kPa and the emissivity from 0.1 to 1.0. Plot the critical heat flux and the temperature rise as functions of the atmospheric pressure and the emissivity, and discuss the results.

10-23 Water is boiled at 1 atm pressure in a 20-cm-internal-diameter teflon-pitted stainless steel pan on an electric range. If it is observed that the water level in the pan drops by 10 cm in 30 min, determine the inner surface temperature of the pan.

Answer: 111.5°C

10-24 Repeat Problem 10-23 for a polished copper pan.

10-25 In a gas-fired boiler, water is boiled at 150°C by hot gases flowing through 50-m-long, 5-cm-outer-diameter mechanically polished stainless steel pipes submerged in water. If the outer surface temperature of the pipes is 165°C, determine (a) the rate of heat transfer from the hot gases to water, (b) the rate of evaporation, (c) the ratio of the critical heat flux to the present heat flux, and (d) the surface temperature of the pipe at which critical heat flux occurs.

Answers: (a) 10,865 kW, (b) 5.139 kg/s, (c) 1.34, (d) 166.5°C

10-26 Repeat Problem 10-25 for a boiling temperature of 160°C.

10-27E Water is boiled at 250°F by a 2-ft-long and 0.5-in.-diameter nickel-plated electric heating element maintained at 280°F. Determine (a) the boiling heat transfer coefficient,

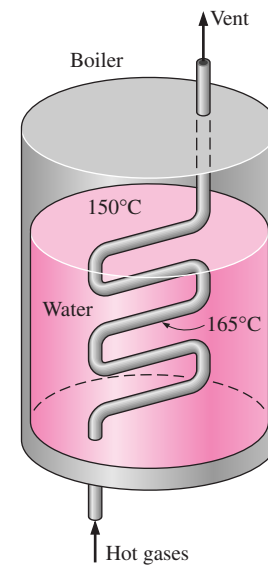



FIGURE P10-25

(b) the electric power consumed by the heating element, and (c) the rate of evaporation of water.


10-28E Repeat Problem 10-27E for a platinum-plated heating element.

10-29E  Reconsider Problem 10-27E. Using EES (or other) software, investigate the effect of surface temperature of the heating element on the boiling heat transfer coefficient, the electric power, and the rate of evaporation of water. Let the surface temperature vary from 260°F to 300°F. Plot the boiling heat transfer coefficient, the electric power consumption, and the rate of evaporation of water as a function of the surface temperature, and discuss the results.

10-30 Cold water enters a steam generator at 15°C and leaves as saturated steam at 100°C. Determine the fraction of heat used to preheat the liquid water from 15°C to the saturation temperature of 100°C in the steam generator.

Answer: 13.6 percent

10-31 Cold water enters a steam generator at 20°C and leaves as saturated steam at the boiler pressure. At what pressure will the amount of heat needed to preheat the water to saturation temperature be equal to the heat needed to vaporize the liquid at the boiler pressure?

10-32  Reconsider Problem 10-31. Using EES (or other) software, plot the boiler pressure as a function of the cold water temperature as the temperature varies from 0°C to 30°C, and discuss the results.

10-33 A 50-cm-long, 2-mm-diameter electric resistance wire submerged in water is used to determine the boiling heat transfer coefficient in water at 1 atm experimentally. The wire temperature is measured to be 130°C when a wattmeter

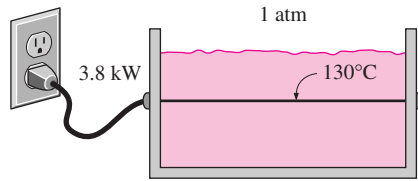


FIGURE P10-33

indicates the electric power consumed to be 3.8 kW. Using Newton's law of cooling, determine the boiling heat transfer coefficient.

Condensation Heat Transfer

10-34C What is condensation? How does it occur?

10-35C What is the difference between film and dropwise condensation? Which is a more effective mechanism of heat transfer?

10-36C In condensate flow, how is the wetted perimeter defined? How does wetted perimeter differ from ordinary perimeter?

10-37C What is the modified latent heat of vaporization? For what is it used? How does it differ from the ordinary latent heat of vaporization?

10-38C Consider film condensation on a vertical plate. Will the heat flux be higher at the top or at the bottom of the plate? Why?

10-39C Consider film condensation on the outer surfaces of a tube whose length is 10 times its diameter. For which orientation of the tube will the heat transfer rate be the highest: horizontal or vertical? Explain. Disregard the base and top surfaces of the tube.

10-40C Consider film condensation on the outer surfaces of four long tubes. For which orientation of the tubes will the condensation heat transfer coefficient be the highest: (a) vertical, (b) horizontal side by side, (c) horizontal but in a vertical tier (directly on top of each other), or (d) a horizontal stack of two tubes high and two tubes wide?

10-41C How does the presence of a noncondensable gas in a vapor influence the condensation heat transfer?

10-42 The Reynolds number for condensate flow is defined as $Re = 4\dot{m}/p\mu_b$, where p is the wetted perimeter. Obtain simplified relations for the Reynolds number by expressing p and \dot{m} by their equivalence for the following geometries: (a) a vertical plate of height L and width w , (b) a tilted plate of height L and width w inclined at an angle θ from the vertical, (c) a vertical cylinder of length L and diameter D , (d) a horizontal cylinder of length L and diameter D , and (e) a sphere of diameter D .

10-43 Consider film condensation on the outer surfaces of N horizontal tubes arranged in a vertical tier. For what value of N

will the average heat transfer coefficient for the entire stack of tubes be equal to half of what it is for a single horizontal tube?

Answer: 16

10-44 Saturated steam at 1 atm condenses on a 3-m-high and 5-m-wide vertical plate that is maintained at 90°C by circulating cooling water through the other side. Determine (a) the rate of heat transfer by condensation to the plate, and (b) the rate at which the condensate drips off the plate at the bottom.

Answers: (a) 942 kW, (b) 0.412 kg/s

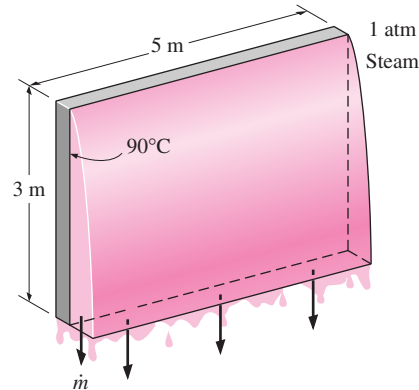


FIGURE P10-44

10-45 Repeat Problem 10-44 for the case of the plate being tilted 60° from the vertical.

10-46 Saturated steam at 30°C condenses on the outside of a 4-cm-outer-diameter, 2-m-long vertical tube. The temperature of the tube is maintained at 20°C by the cooling water. Determine (a) the rate of heat transfer from the steam to the cooling water, (b) the rate of condensation of steam, and (c) the approximate thickness of the liquid film at the bottom of the tube.

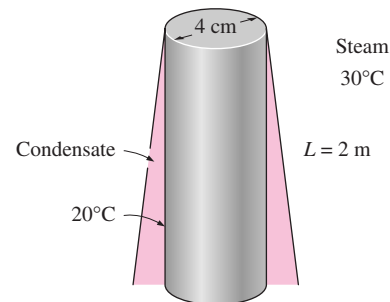


FIGURE P10-46

10-47E Saturated steam at 95°F is condensed on the outer surfaces of an array of horizontal pipes through which cooling water circulates. The outer diameter of the pipes is 1 in. and the outer surfaces of the pipes are maintained at 85°F . Determine (a) the rate of heat transfer to the cooling water circulating in the pipes and (b) the rate of condensation of steam per unit length of a single horizontal pipe.


10-48E Repeat Problem 10-47E for the case of 32 horizontal pipes arranged in a rectangular array of 4 pipes high and 8 pipes wide.

10-49 Saturated steam at 55°C is to be condensed at a rate of 10 kg/h on the outside of a 3-cm-outer-diameter vertical tube whose surface is maintained at 45°C by the cooling water. Determine the tube length required.

10-50 Repeat Problem 10-49 for a horizontal tube.

Answer: 0.70 m

10-51 Saturated steam at 100°C condenses on a 2-m × 2-m plate that is tilted 40° from the vertical. The plate is maintained at 80°C by cooling it from the other side. Determine (a) the average heat transfer coefficient over the entire plate and (b) the rate at which the condensate drips off the plate at the bottom.

10-52  Reconsider Problem 10-51. Using EES (or other) software, investigate the effects of plate temperature and the angle of the plate from the vertical on the average heat transfer coefficient and the rate at which the condensate drips off. Let the plate temperature vary from 40°C to 90°C and the plate angle from 0° to 60°. Plot the heat transfer coefficient and the rate at which the condensate drips off as the functions of the plate temperature and the tilt angle, and discuss the results.

10-53 Saturated ammonia vapor at 10°C condenses on the outside of a 2-cm-outer-diameter, 8-m-long horizontal tube whose outer surface is maintained at -10°C. Determine (a) the rate of heat transfer from the ammonia and (b) the rate of condensation of ammonia.

10-54 The condenser of a steam power plant operates at a pressure of 4.25 kPa. The condenser consists of 100 horizontal tubes arranged in a 10 × 10 square array. The tubes are 8 m

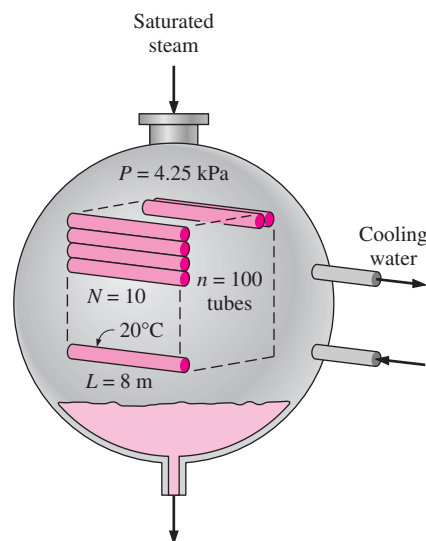



FIGURE P10-54

long and have an outer diameter of 3 cm. If the tube surfaces are at 20°C, determine (a) the rate of heat transfer from the steam to the cooling water and (b) the rate of condensation of steam in the condenser. *Answers: (a) 3678 kW, (b) 1.496 kg/s*


10-55  Reconsider Problem 10-54. Using EES (or other) software, investigate the effect of the condenser pressure on the rate of heat transfer and the rate of condensation of the steam. Let the condenser pressure vary from 3 kPa to 15 kPa. Plot the rate of heat transfer and the rate of condensation of the steam as a function of the condenser pressure, and discuss the results.

10-56 A large heat exchanger has several columns of tubes, with 20 tubes in each column. The outer diameter of the tubes is 1.5 cm. Saturated steam at 50°C condenses on the outer surfaces of the tubes, which are maintained at 20°C. Determine (a) the average heat transfer coefficient and (b) the rate of condensation of steam per m length of a column.

10-57 Saturated refrigerant-134a vapor at 30°C is to be condensed in a 5-m-long, 1-cm-diameter horizontal tube that is maintained at a temperature of 20°C. If the refrigerant enters the tube at a rate of 2.5 kg/min, determine the fraction of the refrigerant that will have condensed at the end of the tube.

10-58 Repeat Problem 10-57 for a tube length of 8 m.

Answer: 17.2 percent

10-59  Reconsider Problem 10-57. Using EES (or other) software, plot the fraction of the refrigerant condensed at the end of the tube as a function of the temperature of the saturated R-134a vapor as the temperature varies from 25°C to 50°C, and discuss the results.

Special Topic: Heat Pipes

10-60C What is a heat pipe? How does it operate? Does it have any moving parts?

10-61C A heat pipe with water as the working fluid is said to have an effective thermal conductivity of 100,000 W/m · °C, which is more than 100,000 times the conductivity of water. How can this happen?

10-62C What is the effect of a small amount of noncondensable gas such as air on the performance of a heat pipe?

10-63C Why do water-based heat pipes used in the cooling of electronic equipment operate below atmospheric pressure?

10-64C What happens when the wick of a heat pipe is too coarse or too fine?

10-65C Does the orientation of a heat pipe affect its performance? Does it matter if the evaporator end of the heat pipe is up or down? Explain.

10-66C How can the liquid in a heat pipe move up against gravity without a pump? For heat pipes that work against gravity, is it better to have coarse or fine wicks? Why?

10-67C What are the important considerations in the design and manufacture of heat pipes?

10-68C What is the major cause for the premature degradation of the performance of some heat pipes?

10-69 A 40-cm-long cylindrical heat pipe having a diameter of 0.5 cm is dissipating heat at a rate of 150 W, with a temperature difference of 4°C across the heat pipe. If we were to use a 40-cm-long copper rod ($k = 386 \text{ W/m} \cdot ^\circ\text{C}$ and $\rho = 8950 \text{ kg/m}^3$) instead to remove heat at the same rate, determine the diameter and the mass of the copper rod that needs to be installed.

10-70 Repeat Problem 10-69 for an aluminum rod instead of copper.

10-71E A plate that supports 10 power transistors, each dissipating 35 W, is to be cooled with 1-ft-long heat pipes having a diameter of $\frac{1}{4}$ in. Using Table 10-6, determine how many pipes need to be attached to this plate. *Answer: 2*

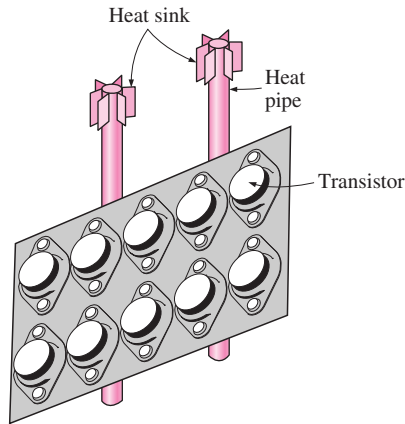


FIGURE P10-71E

Review Problems

10-72 Steam at 40°C condenses on the outside of a 3-cm diameter thin horizontal copper tube by cooling water that enters the tube at 25°C at an average velocity of 2 m/s and leaves at 35°C. Determine the rate of condensation of steam, the average overall heat transfer coefficient between the steam and the cooling water, and the tube length.

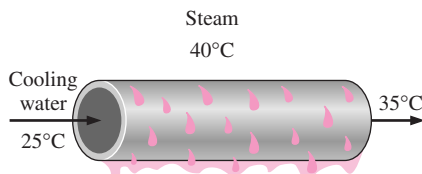


FIGURE P10-72

10-73 Saturated ammonia vapor at 25°C condenses on the outside of a 2-m-long, 3.2-cm-outer-diameter vertical tube maintained at 15°C. Determine (a) the average heat transfer

coefficient, (b) the rate of heat transfer, and (c) the rate of condensation of ammonia.

10-74 Saturated isobutane vapor in a binary geothermal power plant is to be condensed outside an array of eight horizontal tubes. Determine the ratio of the condensation rate for the cases of the tubes being arranged in a horizontal tier versus in a vertical tier of horizontal tubes. *Answer: 1.68*

10-75E The condenser of a steam power plant operates at a pressure of 0.95 psia. The condenser consists of 144 horizontal tubes arranged in a 12×12 square array. The tubes are 15 ft long and have an outer diameter of 1.2 in. If the outer surfaces of the tubes are maintained at 80°F, determine (a) the rate of heat transfer from the steam to the cooling water and (b) the rate of condensation of steam in the condenser.

10-76E Repeat Problem 10-75E for a tube diameter of 2 in.

10-77 Water is boiled at 100°C electrically by a 80-cm-long, 2-mm-diameter horizontal resistance wire made of chemically etched stainless steel. Determine (a) the rate of heat transfer to the water and the rate of evaporation of water if the temperature of the wire is 115°C and (b) the maximum rate of evaporation in the nucleate boiling regime.

Answers: (a) 2387 W, 3.81 kg/h, (b) 1280 kW/m²

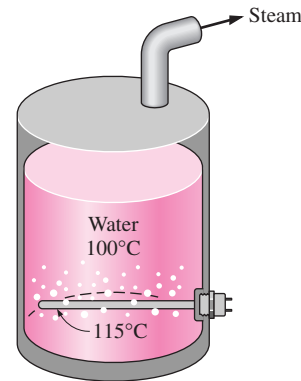


FIGURE P10-77

10-78E Saturated steam at 100°F is condensed on a 6-ft-high vertical plate that is maintained at 80°F. Determine the rate of heat transfer from the steam to the plate and the rate of condensation per foot width of the plate.


10-79 Saturated refrigerant-134a vapor at 35°C is to be condensed on the outer surface of a 7-m-long, 1.5-cm-diameter horizontal tube that is maintained at a temperature of 25°C. Determine the rate at which the refrigerant will condense, in kg/min.

10-80 Repeat Problem 10-79 for a tube diameter of 3 cm.

10-81 Saturated steam at 270.1 kPa condenses inside a horizontal, 6-m-long, 3-cm-internal-diameter pipe whose surface is maintained at 110°C. Assuming low vapor velocity, determine

the average heat transfer coefficient and the rate of condensation of the steam inside the pipe.

Answers: 3345 W/m² · °C, 0.0174 kg/s

10-82  A 1.5-cm-diameter silver sphere initially at 30°C is suspended in a room filled with saturated steam at 100°C. Using the lumped system analysis, determine how long it will take for the temperature of the ball to rise to 50°C. Also, determine the amount of steam that condenses during this process and verify that the lumped system analysis is applicable.

10-83 Repeat Problem 10-82 for a 3-cm-diameter copper ball.

10-84 You have probably noticed that water vapor that condenses on a canned drink slides down, clearing the surface for further condensation. Therefore, condensation in this case can be considered to be dropwise. Determine the condensation heat transfer coefficient on a cold canned drink at 5°C that is placed in a large container filled with saturated steam at 95°C.



FIGURE P10-84

10-85 A resistance heater made of 2-mm-diameter nickel wire is used to heat water at 1 atm pressure. Determine the highest temperature at which this heater can operate safely without the danger of burning out. *Answer: 109.6°C*

Computer, Design, and Essay Problems

10-86 Design the condenser of a steam power plant that has a thermal efficiency of 40 percent and generates 10 MW of net electric power. Steam enters the condenser as saturated vapor at 10 kPa, and it is to be condensed outside horizontal tubes through which cooling water from a nearby river flows. The temperature rise of the cooling water is limited to 8°C, and the velocity of the cooling water in the pipes is limited to 6 m/s to keep the pressure drop at an acceptable level. Specify the pipe diameter, total pipe length, and the arrangement of the pipes to minimize the condenser volume.

10-87 The refrigerant in a household refrigerator is condensed as it flows through the coil that is typically placed

behind the refrigerator. Heat transfer from the outer surface of the coil to the surroundings is by natural convection and radiation. Obtaining information about the operating conditions of the refrigerator, including the pressures and temperatures of the refrigerant at the inlet and the exit of the coil, show that the coil is selected properly, and determine the safety margin in the selection.

10-88 Water-cooled steam condensers are commonly used in steam power plants. Obtain information about water-cooled steam condensers by doing a literature search on the topic and also by contacting some condenser manufacturers. In a report, describe the various types, the way they are designed, the limitation on each type, and the selection criteria.

10-89 Steam boilers have long been used to provide process heat as well as to generate power. Write an essay on the history of steam boilers and the evolution of modern supercritical steam power plants. What was the role of the American Society of Mechanical Engineers in this development?

10-90 The technology for power generation using geothermal energy is well established, and numerous geothermal power plants throughout the world are currently generating electricity economically. Binary geothermal plants utilize a volatile secondary fluid such as isobutane, n-pentane, and R-114 in a closed loop. Consider a binary geothermal plant with R-114 as the working fluid that is flowing at a rate of 600 kg/s. The R-114 is vaporized in a boiler at 115°C by the geothermal fluid that enters at 165°C and is condensed at 30°C outside the tubes by cooling water that enters the tubes at 18°C. Design the condenser of this binary plant.

Specify (a) the length, diameter, and number of tubes and their arrangement in the condenser, (b) the mass flow rate of cooling water, and (c) the flow rate of make-up water needed if a cooling tower is used to reject the waste heat from the cooling water. The liquid velocity is to remain under 6 m/s and the length of the tubes is limited to 8 m.

10-91 A manufacturing facility requires saturated steam at 120°C at a rate of 1.2 kg/min. Design an electric steam boiler for this purpose under these constraints:

- The boiler will be in cylindrical shape with a height-to-diameter ratio of 1.5. The boiler can be horizontal or vertical.

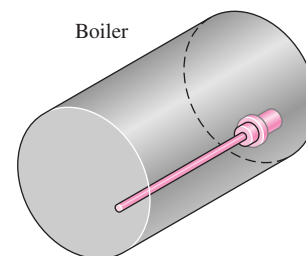


FIGURE P10-91

- The boiler will operate in the nucleate boiling regime, and the design heat flux will not exceed 60 percent of the critical heat flux to provide an adequate safety margin.
- A commercially available plug-in type electrical heating element made of mechanically polished stainless steel will be used. The diameter of the heater cannot be between 0.5 cm and 3 cm.
- Half of the volume of the boiler should be occupied by steam, and the boiler should be large enough to hold enough water for 2 h supply of steam. Also, the boiler will be well insulated.

You are to specify the following: (1) The height and inner diameter of the tank, (2) the length, diameter, power rating, and surface temperature of the electric heating element, (3) the maximum rate of steam production during short periods of overload conditions, and how it can be accomplished.

10-92 Repeat Problem 10-91 for a boiler that produces steam at 150°C at a rate of 2.5 kg/min.

10-93 Conduct this experiment to determine the boiling heat transfer coefficient. You will need a portable immersion-type electric heating element, an indoor-outdoor thermometer, and metal glue (all can be purchased for about \$15 in a hardware store). You will also need a piece of string and a ruler to calcu-

late the surface area of the heater. First, boil water in a pan using the heating element and measure the temperature of the boiling water away from the heating element. Based on your reading, estimate the elevation of your location, and compare it to the actual value. Then glue the tip of the thermocouple wire of the thermometer to the midsection of the heater surface. The temperature reading in this case will give the surface temperature of the heater. Assuming the rated power of the heater to be the actual power consumption during heating (you can check this by measuring the electric current and voltage), calculate the heat transfer coefficients from Newton's law of cooling.

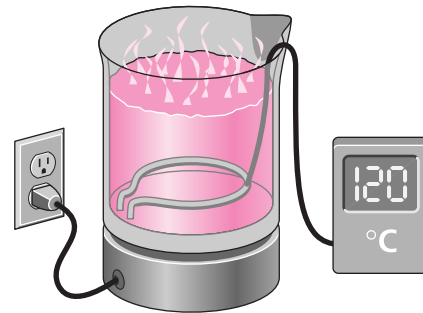


FIGURE P10-93